Climate Politics in the United States*

Matilde Bombardini
UC-Berkeley

Frederico Finan
UC-Berkeley

Nicolas Longuet-Marx
Stanford University

Suresh Naidu
Columbia University

Francesco Trebbi
UC-Berkeley

July 12, 2025

Abstract

We study the effects of climate change and mitigation-related employment changes on U.S. politics. We combine 2000-2020 precinct-level voting information and congressional candidate positions on environmental policy with high-resolution temperature and precipitation data and census block-group level measures of "green" and "brown" employment shares. Holding politician positions fixed within a district, we find that Democratic vote share increases with exogenous changes in local climate and green transition employment. We embed these estimates into a structural model of political competition, including both direct and demand-driven effects of shocks on candidate policy platform supply. Incorporating our model estimates into 2022-2050 projections of climate change and green employment transition, we find that voting for the Democratic Party increases, while both parties move slightly to the *right* on climate policy. Under worst-case climate projections and current mitigation trajectories, our estimates indicate that the probability the House passes a carbon-pricing bill is 9 percentage points higher in 2050 than in 2020.

*Bombardini: UC Berkeley and National Bureau of Economic Research (mbombardini@berkeley.edu). Finan: UC Berkeley and National Bureau of Economic Research (ffinan@berkeley.edu). Longuet-Marx: Stanford Institute for Economic Policy Research (nicolas.longuetmarx@stanford.edu). Naidu: Columbia University and National Bureau of Economic Research (sn2430@columbia.edu). Trebbi: UC Berkeley and National Bureau of Economic Research (ftrebbi@berkeley.edu). Aidan Wang, Ming-Yen Ho, and Ziyi Liu provided exceptional research assistance. We thank Judd Boomhower, Bard Harstad, Kelsey Jack, Andrea Prat, Mounu Prem, Silvia Vannutelli, Reed Walker, seminar and conference participants at Columbia, BFI-IOG meeting Summer 2024, Bocconi, CEMFI, EIEF, and Stanford for comments and suggestions.

1 Introduction

Climate change is recognized as having large effects on economic well-being. A substantial and growing literature shows effects of temperature, weather, and extreme environmental events on mortality, GDP, health, crime, schooling, job quality, and civil strife (Dell, Jones and Olken, 2012; Carleton et al., 2022; Burke et al., 2023). Scientists and economists have proposed many policies, from carbon pricing to green technology subsidies, that could potentially slow global warming (Hahn et al., 2024). Yet many of these policies have not been widely implemented, or have been passed and subsequently rejected by voters in democratic elections (Doyle, McEachern and MacGregor, 2015; Rowan, 2023). Climate adaptation also remains limited (Burke et al., 2024). It has become increasingly clear that understanding voting and endogenous policy-setting is important for successfully tackling climate change in democratic countries (Dechezleprêtre et al., 2022). Politics, rather than just technology, appears to be a fundamental barrier to climate action.[1] But there is surprisingly little research on how climate change affects democratic politics, and most projections of future impacts overlook political economy considerations.

With this motivation, our paper focuses on the political economy of climate change. We empirically document the effects of weather shocks and mitigation-related employment changes on partisan voting and political competition over environmental policy in the U.S. Specifically, we use a new panel of precinct-level voting data to estimate how extreme temperature and precipitation shocks, as well as employment in "green" and "brown" jobs, affect vote shares. We then combine these within-district estimates with new data on candidate positions on environmental issues to build and estimate a demand and supply system of electoral competition over climate policy at the congressional district level. Using this structural model, we assess the effects of projected climate-change scenarios on electoral politics and congressional policy-making for the years 2022-2050.

Analyzing the political economy of climate change presents several complex econometric challenges. It is difficult to identify the drivers of voter demand for climate action and to quantify how much this demand matters in equilibrium. The absence of strong climate policy may reflect low voter demand, potentially due to limited awareness, misinformation, or uncertainty about the costs of climate change. Alternatively,

[1] Some scholarship has even questioned whether democratic institutions may be suitable to tackle such a complex, forward-looking task given their many veto points. In the words of Lazar and Wallace (2025) *"Governments have been slow to respond to climate change, slow to prevent further damage to our atmosphere, and slow to prepare for what is coming. Democratic governments, it is sometimes said, are worst of all at these tasks."* (p.135)

voters may fear the economic burden of transitioning to a low-carbon society. Low demand may also stem from increasing ideological and partisan polarization, which exposes climate policy to the same gridlock affecting other policy domains.[2] Furthermore, from an econometric perspective, canonical models of electoral competition imply that identifying voter demand parameters requires controlling for candidates' policy positions, which themselves depend on expected vote shares.

To address these challenges on the voter demand side, we estimate the relationship between Democratic vote margins and extreme weather events, as measured by the average number of days in which the temperature and precipitation were two standard deviations above their historical averages. Because employment is central to the political economy of climate policy, we also examine how the local employment share in green (low-carbon) and brown (high-carbon) industries affects vote choice. To identify these effects, we construct a new 20-year panel dataset at the census block-group that links voting, climate, and employment data. The granularity of the data together with its panel structure allows us to estimate highly-localized effects, while controlling for key confounders—such as candidate platforms or geographic sorting—that often bias estimates relying on cross-sectional or more aggregated data.

We find that both climate shocks and employment composition significantly influence Democratic vote margins. Under our preferred specification, a one standard deviation increase in extreme heat days (8.13 days) increases the Democratic margin by 0.90 percentage points. A one standard deviation increase in extreme precipitation (6.74 days) yields a smaller, less significant 0.35 percentage point increase. Regarding employment, a one standard deviation rise in brown job share (1.75 percentage points) decreases the Democratic margin by 0.62 percentage points, while a similar increase in green jobs boosts it by 0.34 percentage points. Together, our results suggest that weather and employment shocks have comparable effects on voter support for Democratic candidates.

Our findings are robust to multiple specification checks, including alternative climate variable constructions, varying sets of fixed effects, spatial autocorrelation adjustments, and a rich set of time-varying socio-demographic controls. To address potential endogeneity in local job composition, we also implement a shift-share instrument following Borusyak, Hull and Jaravel (2022), yielding similar results. Finally, we show that electoral effects are more pronounced in contests where environmental issues are salient—such as Texas Railroad Commission races—supporting the interpretation that these effects are driven by climate policy preferences rather than general partisan shifts.

[2]See Voorheis, McCarty and Shor (2015); Binder (2004).

We then investigate how the same climate and employment shocks affect the environmental platforms adopted by political candidates, controlling for voter demand. One reason long-term projections of climate politics are difficult is that the electoral landscape itself evolves over time (Calvo, Pons and Shapiro, 2024), underscoring the importance of modeling not just demand, but also the supply of climate policies. In some cases, the absence of strong climate policy may reflect limited policy supply, even in the presence of high voter demand. Climate issues may be "bad politics" given the structure of electoral competition (e.g., due to the location of swing districts, donor or concentrated electoral blocs) or other legislative incentives (e.g., bargaining over other issues).[3]

For our supply-side analysis, we measure environmental policy platforms for both winners and losers of congressional races using campaign websites and candidate surveys collected by Longuet-Marx (2024). We show that these campaign-based environmental ideal points strongly correlate with subsequent roll-call votes on climate policy among elected officials, indicating that campaign platforms credibly signal true policy preferences. While political science and political economy have long relied on multidimensional scaling models to measure policy preferences of politicians (Poole and Rosenthal (2011), Clinton, Jackman and Rivers (2004), McCarty, Poole and Rosenthal (2016), Canen, Kendall and Trebbi (2020), Canen, Kendall and Trebbi (2021)), these approaches typically focus on incumbents, limiting their usefulness for studying electoral competition.[4]

To analyze supply-side behavior, we model electoral competition using a standard probabilistic voting model, which provides the microfoundations for a streamlined supply-and-demand framework that we then estimate using GMM. Crucially, this framework allows us to not only recover politically salient parameters—such as the responsiveness of candidate platforms to expected vote shares—but to forecast political equilibria under different climate change scenarios.

Our simulations reveal that under the most extreme climate scenario, Democratic vote shares increase. Yet, both parties shift slightly *rightward* on climate policy. Despite this, Democratic gains shift the composition of Congress enough that, by 2050,

[3]Relatively fewer studies have focused on the supply side of environmental policy by political parties, with exceptions including List and Sturm (2006); Fredriksson, Wang and Mamun (2011); Aklin and Urpelainen (2013); Béland and Boucher (2015); Gagliarducci, Paserman and Patacchini (2019); Kaplan, Spenkuch and Yuan (2019). Our paper contributes to this literature by jointly modeling the interaction between voter demand and policy supply in response to climate change.

[4]An exception is the method in Bonica (2013) to estimate ideal points from Political Action Committee contributions. These ideal points can be calculated for all candidates in a race with available political donations data.

the environmental roll-call position of the median legislator is significantly more pro-climate than today, raising the probability of voting for emissions pricing by 9 percentage points.[5]

While these forecasts are inherently uncertain, they offer a proof of concept for quantitatively integrating political economy dynamics into long-run climate models and economic estimates of carbon costs. Existing frameworks—particularly most Integrated Assessment Models (IAMs)—typically link climate projections with economic variables, but omit political feedback loops. In this sense, our approach aligns most closely with Moore et al. (2022), who incorporate reduced-form political feedbacks, social conformity, and endogenous technology adoption into a climate model. Their model imposes a threshold: climate policy only emerges when supporters outnumber opponents. In contrast, we adopt a structural political economy framework that microfounds policy outcomes as the result of interactions between voter preferences and electoral competition in equilibrium.

Our paper contributes to several strands of literature. It broadly relates to a large literature in economics and political science that has examined voter beliefs and preferences regarding climate policy, including in response to climate and weather shocks, which mostly focuses on survey evidence.

In an influential contribution, Egan and Mullin (2012) studies public opinion data from Pew Research Center as a response to severe weather shocks. The authors show that "*weather patterns have a significant effect on people's beliefs about the evidence for global warming.*" Similar results are also in Deryugina (2013) or Bergquist and Warshaw (2019). The evidence since then has been more mixed (Egan and Mullin, 2017). Hilbig and Riaz (2024) present precise zeros in estimating the effects of flooding in Germany, focusing on voter beliefs about climate change and electoral support for the Green Party in federal elections. These results appear in contrast with Hoffmann et al. (2022), that also study Green Parties in Europe, but find positive effects.[6]

We speak more directly to a smaller literature that has analyzed actual voting behavior in response to climate shocks, with notable exceptions including Healy and Malhotra (2010); Gasper and Reeves (2011); Stokes (2016); Pahontu (2020); Boomhower (2024), and a handful of papers on Green Party support in Europe (Hoffmann et al., 2022; Hilbig and Riaz, 2024). Both ballot initiatives and elections for state office and

[5]For reference, the 2009 Waxman-Markey bill to establish a national cap-and-trade system passed the House with support from 83% of Democrats (211 of 255) and only 8 Republicans. The bill aimed to reduce emissions by 83% by 2050. `https://www.nytimes.com/2009/06/27/us/politics/27climate.html`

[6]A recent paper looking at the effect of disasters on roll-call voting in the U.S. Congress finds that only Democrats support more green legislation (Jud and Nguyen, 2024).

legislatures have been studied, but not extensively, and mostly with a focus on the demand side. Kahn and Matsusaka (1997) focus on 16 ballot initiatives in California and estimates a county voter demand model, finding that environmental policy appears a normal good for most voters. List and Sturm (2006) focus on single-issue environmental voters in U.S. gubernatorial elections. Stokes (2016) focuses on voter backlash to costly environmental projects (NIMBY wind turbine location) in Canada, whereas Urpelainen and Zhang (2022) show that U.S. wind development raises Democratic vote share. Anderson, Marinescu and Shor (2023) study two failed carbon tax referenda in Washington State in 2016 and 2018 and emphasize how ideology explains much of the variation in voting outcomes, a result in sharp contrast with conclusions in Kahn and Matsusaka (1997), where voter ideology is deemed less relevant. Closer to our approach in terms of identifying variation of demand parameters, Hazlett and Mildenberger (2020) focus on the political consequences of wildfire exposure on voting, showing that wildfires increase support for costly pro-climate ballot initiatives by 5 to 6 percentage points for Californians living within 5 kilometers of a recent wildfire, but find an asymmetry between Democratic and Republican localities. Boomhower (2024) focuses on the electoral consequences of earthquakes induced by fracking activities in the states of Oklahoma and Texas. The author focuses on environmental regulators, who are elected (not appointed) in those states, and finds compelling causal evidence of lower support for incumbents and higher turnout after a local shock.

Our paper also speaks to a new and growing literature on the structural estimation of electoral demand models. Examples include Berry, Cox and Haile (2024), and equilibrium systems of demand and supply such as Longuet-Marx (2024); Cox (2024); Iaryczower, Montero and Kim (2022). We complement these recent papers through a specific focus on climate politics, which lends the structural model to novel quantitative applications within the space of climate projections. By necessity, our equilibrium model is also more streamlined and parsimonious than some of these alternatives, as the model has to be solved forward in order to deliver quantitative projections from 2022 up to 2050.

These projections are also a new contribution of the paper. We provide a microfounded, quantitative approach for integrating political economy forces in climate forecasting and potentially useful for extending Integrated Assessment Models (IAMs) (Wiliam and Thompson (2017); Geels, Berkhout and Van Vuuren (2016)). IAMs could benefit from incorporating an explicitly endogenous policy-making process, and, as discussed above, our quantitative equilibrium model of climate politics can complement the more reduced-form approaches that have been proposed in the climate science literature.

In the next section, we describe the data. We then present our demand estimates using within-congressional district variation, along with heterogeneity and robustness exercises. We then present our empirical model of political competition and endogenous supply of environmental policy, and discuss identification and consistency with the demand estimates. We then discuss results from the unified model of political equilibrium, with both demand and supply estimates. Finally, we integrate climate projection data with our structural estimates and project various future scenarios for how climate change will change the composition and ideology of the U.S. House of Representatives. The last section concludes.

2 Data

This section presents an overview of the main data sources used in the paper. All the details of the data construction can be found in the Online Appendix.

Electoral Voting Data: We use precinct-level voting data from Longuet-Marx (2024). Precincts are the smallest level at which election results are reported in the United States. A precinct has on average 1,200 registered voters, that is, on average, 60 times smaller than a county and 400 times smaller than a congressional district. Since precinct boundaries change over time, in order to build a stable panel of geographic subunits of a congressional district, we assign all precinct votes to the 2010 census block-group level as our geographic unit (see Longuet-Marx (2024) for details). Block-groups have approximately the same population size as a precinct, and a census block-group is a geographical unit used by the U.S. Census Bureau for collecting and reporting demographic data. It is a subdivision of a census tract that is divided into census blocks. We also obtain block-group-level demographics from the decennial U.S. Census and the American Community Survey (ACS) for each election.

Climate: Our primary data for temperature and precipitation come from an updated version of Schlenker and Roberts (2009), which reports daily minimum temperature, maximum temperature, and total precipitation on each 2.5 mile $\times$ 2.5 mile grid cell for the contiguous U.S. At the grid-cell level, we first construct weather measurements as follows. First, we calculate the mean and standard deviation of average daily temperature (maximum plus minimum temperature of the day divided by two) and precipitation for each calendar day of the year (January 1st, ... , December 31st) between 1959 and 1999. For each grid cell starting in 2000, a day's average temperature or precipitation is considered to be extreme if the day's temperature or precipitation

exceeds the historical average for that day by two historical standard deviations. Aggregating to the year level, we count the total number of days with extreme temperature and precipitation for each year from 2000 to 2020. We also count the number of days that exceeds a number of temperature and precipitation thresholds (e.g., 30 degrees Celsius), total precipitation, and average temperature of the year, and various temperature and precipitation bins indicating the number of days with temperature and precipitation within a fixed range for each grid cell.

To aggregate grid cell-by-year-level data to census block-group and congressional district level, we first match each census block's centroid to the four closest grid cells. The census block's estimated days with extreme temperature, precipitation, and other weather variables are the weighted average of the corresponding variables for the linked grid cells, inversely weighted by the grid cell's distance to the census block centroid. We then aggregate block-gorup-level data to the block-group level by taking a population-weighted average of block-group-level variables.

Candidate Positions on the Environment: We use the campaign environmental ideal points calculated in Longuet-Marx (2024). These policy positions are calculated by combining text data from candidate official websites obtained from the Library of Congress with candidate survey information from Project Vote Smart, a non-partisan organization that collects and distributes information on candidates running for public office in the U.S. and whose data has long been used in the political science and political economy literature (Ansolabehere, Snyder Jr and Stewart III, 2001).[7] Candidate ideal points are estimated using a Bayesian item response model applied to environment-related questions from the Vote Smart survey. These scores are then predicted for all candidates using the text from their campaign websites, thus ensuring complete coverage across both winners and losers. We also compute environment-specific ideal points based on roll-call votes for winning candidates in Congress, following Bateman and Lapinski (2016) and Kuziemko, Longuet-Marx and Naidu (2023), restricting the estimation to bills that the Comparative Agendas Project (CAP) codes as environmental. These ideal points measure the latent probability that a candidate votes "yes" on a right-wing environmental bill, given the voting behavior of other legislators. Appendix Figure A.15 shows that for winners, roll-call votes made in Congress on environmental bills are significantly correlated with the campaign ideal points used in our analysis.

[7]See the Political Courage Test (formerly the National Political Awareness Test, NPAT) https://www.votesmart.org/.

Green and Brown Jobs: We construct a measure of employment in"green" jobs for residents of a block-group by combining multiple data sources. We adopt a definition of green jobs based on the Bureau of Labor Statistics (BLS) Green Goods and Services (GGS) survey, conducted in 2011. We use their classification of green NAICS 6-digit industries, which are those that produce goods or services that "benefit the environment or conserve natural resources." The BLS GGS also provides a share of employment, within each of those industries, that is deemed to be devoted to green activities. Ideally, we would observe each block-group b's residents employment in a NAICS 6-digit industry. Lacking such detailed industry employment information, we approximate $GreenEmp_{bt}$ as detailed in Appendix section B.2 using data on: i) block-group employment at NAICS 2-digit level from the Decennial Census and the Census LEHD Origin-Destination Employment Statistics (LODES) Residence Area Characteristics (RAC) dataset; ii) commuting flows from block-groups to counties at a super-sector level from the LODES Origin-Destination (OD) dataset; iii) county employment by NAICS 6-digit from the County Business Patterns (CBP) and the BLS Quarterly Census of Employment and Wages (QCEW). The logic behind this approximation is that, while we know b's residents' NAICS 2-digit sector of employment, we do not know which specific NAICS 6-digit industry employs them. Therefore we attribute the industry based on commuting to jobs in potentially different counties and those counties' shares of green employment within each NAICS 2-digit industry. In this process we employ a constrained imputation method analogous to Autor et al. (2024), detailed in the Online Appendix.[8]

The construction of the number of "brown" jobs in block-group b is analogous to that of green jobs. We classify as brown jobs those easily recognizable as related to oil and gas extraction, coal mining and their support activities (OGC). The list of eight 6-digit NAICS industries can be found in Appendix Section B.2, but they are all within NAICS 2-digit industry 21 "Mining, Quarrying, and Oil and Gas Extraction".

The geographic variation in our main variables is illustrated in the maps of Figure 1. There is clear evidence of spatial correlation in voting patterns, weather changes, and employment changes.

Projections of Future Climate: Data for the weather projections come from the NASA Earth Exchange (NEX) Global Daily Downscaled Projections (GDDP) dataset. The NEX-GDDP dataset contains daily average temperature and precipitation projections from 2015 up to year 2100 at the resolution of 25km $\times$ 25km (0.25 $\times$ 0.25

[8]We especially thank David Dorn for suggestions and sharing details about the code.

degrees in latitude × longitude) grids coming from different climate models of the 6th generation of the Coupled Model Intercomparison Project (CMIP6). We use the projections of Community Earth System Model 2 (CESM2), developed and maintained by the NSF's National Center for Atmospheric Research (NCAR).

All NEX-GDDP models, including CESM-2, projected outcomes correspond to four different "Shared Socioeconomic Pathway" (SSP) scenarios, named SSP1-2.6, SSP2-4.5, SSP3-7.0, and SSP5-8.5. Each SSP predicts how a different set of socioeconomic and policy responses could influence climate outcomes. SSP5-8.5 reflects a worst case "business as usual" where carbon emissions continue to increase along with historical trends without policy mitigation. SSP3-7.0 is a "middle of the road" outcome with still no climate policies, but milder increases in emissions relative to SSP5-8.5. SSP2-4.5 corresponds to a scenario where policy successfully restricted global warming to be below 3C by year 2100, while SSP1-2.6 reflects an "optimistic" outcome where warming will be below 2C. Each model × scenario is a dataset at the day × latitude-longitude grid cell level, describing the temperature and precipitation at the grid cell for each day of the year from 2024 to 2050.

We build a congressional district × election year level dataset of weather variables (average temperature, total precipitation, days of extreme temperature and precipitation) by comparing the projected temperature with historical means under each scenario.

Projected Jobs Data: For job projections, we use the BLS Occupational Outlook Handbook (BLS OOH), which projects job growth between 2023 and 2033 for various NAICS code sectors at the 3 to 6 digit levels. We construct the annualized growth rate of each 6 digit 2012 NAICS sector using the 2012-2022 NAICS crosswalk.[9]

Starting with our data of brown and green jobs at the block-group × 6 digit NAICS sector level in 2021, we construct the growth rate of brown and green jobs for each block-group between 2023 and 2033 by taking a weighted average of the BLS OOH growth rate for each 6-digit NAICS sector, weighted by the current importance of each sector in that block-group. For example, the annualized growth rate of green employment in block-group b is:

$$GreenGrowth_{bt} = \frac{\sum_i^I GrowthRate_{it} \times GreenEmp_{bi,2021}}{\sum_i^I GreenEmp_{bi,2021}} \tag{1}$$

where i indexes a 6-digit NAICS sector and $\text{GreenEmp}_{bi,2021}$ is the number of green

[9]https://www.bls.gov/cew/classifications/industry/qcew-naics-hierarchy-crosswalk.htm

jobs for sector i in block-group b in year 2021.

We predict the growth rate of block-group-level total employment with the same method by aggregating all sectors, which gives us the growth rate of the proportion of green and brown jobs in each block-group. We then aggregate these to the congressional district level.

The time-series averages of our variables and their projections are plotted in Appendix Figure A.17. The BLS projects only a modest rise in the green-job share and an equally modest decline in oil, gas, and coal employment over the next decade. The geographic distribution projected in 2050 is presented in the maps in Figure A.18.

3 Voter Demand Specification

In this section, we begin by examining the reduced-form effects of climate variation on voting patterns. We then extend our demand specification to incorporate the influence of green and brown employment. In addition to a range of robustness checks, we analyze elections for energy regulators, races that are arguably focused almost exclusively on environmental issues. Finally, we conclude with an analysis of demand heterogeneity as implied by models of political competition.

We follow the climate-economy literature and include fine geographic (in our case census block-group) fixed effects, as well as coarser geography by time fixed effects. Our baseline specification is given by:

$$y_{bt} = \delta^{temp} Temp_{bt} + \delta^{prec} Precip_{bt} + \alpha X_{bt} + \mu_b + \Omega_{c(b),t} + \epsilon_{bt} \tag{2}$$

where y_{bt} is the share of votes cast for the Democratic candidate minus the share of votes cast for the Republican candidate in block-group b in election year t. Recall that a block-group is the stable geographic unit that we employ. $Temp_{bt}$ and $Precip_{bt}$ are measures of temperature and precipitation in block-group b and election year t as described in Section 2. Let μ_b indicate block-group fixed effects, which absorb time-invariant heterogeneity. We refer to $c(b)$ as the congressional district to which b belongs. $\Omega_{c(b),t}$ are congressional district $\times$ election year fixed effects, and absorb all the variation coming from candidates and campaigns, as well as other sources of time-varying heterogeneity at the broader geographic level of a congressional district. More precisely, as congressional district boundaries change due to redistricting after each Decennial Census, by congressional district c we intend the geographic unit defined by a congressional district per redistricting cycle. We will use the term congressional district for brevity whenever it is not confusing.

It is important to note that the remaining variation in weather shocks across block-groups after introducing congressional district × election year fixed effects is still substantial. This residual weather variance represents different shares of the overall variation in temperature and precipitation shocks in different states: Appendix figures A.8 reports such residual variation shares varying from 3.4% in Illinois to 55.6% in Montana for temperature. In X_{bt} we include time-varying sets of controls, and we cluster our standard errors both at the congressional district $c(b)$ by election t level and at the block-group level b.

While the exogeneity of weather shocks allows us to obtain unbiased reduced-form estimates of the parameters δ^{temp} and δ^{prec}, a remaining concern is that these estimates may reflect indirect effects, such as those operating through geographic sorting, rather than the direct impact of climate shocks on voting. However, there are at least two reasons why this is unlikely in our context. First, we focus on short-term weather fluctuations within two-year election cycles, a time frame too narrow for extreme weather events to plausibly induce significant selective migration. Second, as we show later, our results are robust to controlling for a wide set of time-varying observables. These include the shares of the population that are wage earners, veterans, secondary- and tertiary-educated, English-speaking, self-employed, rural, retired, never married, native-born, or married, as well as those working in finance, education, health, the armed forces, and manufacturing. We also control for the mean of log income, log employment, and voting-age population.

3.1 Climate Results

Figure 2 presents binned scatter plots based on equation (2), controlling for block-group fixed effects and congressional district × election year fixed effects. The data reveal a clear positive relationship between Democratic vote margin and our weather variables, with temperature showing a slightly tighter fit than precipitation.

Table 1 explores the robustness of these relationships. Column 1 adds an extensive set of time-varying block-group-level controls, while column 2 further includes media market (DMA) × election year fixed effects to account for climate effects driven by differential media exposure.

The coefficients remain robust and economically meaningful. A one standard deviation increase in extreme temperature days (defined as days above two standard deviations from the historical average, or 8.13 days) is associated with a 0.66 percentage point increase in Democratic vote margin (column 1). For context, this effect is comparable to 2.5 additional minutes of weekly Fox News exposure (Martin and

Yurukoglu, 2017), or slightly exceeds one standard deviation in partisan advertising intensity (Spenkuch and Toniatti, 2018). While smaller, the effect of precipitation is also politically relevant: a one standard deviation increase (6.74 days) raises the Democratic vote margin by 0.35 percentage points. Taken together, our climate variables suggest that a one standard deviation shock increases Democratic margins by 0.94 percentage points.

In columns 3 and 4, we exclude block-group fixed effects. Column 4 also includes a time-varying sixth-degree polynomial in latitude and longitude (with interactions). These specifications rely solely on within–congressional district-year variation to identify climate effects. This change has two implications: first, because block-groups are geographically small, these specifications allow for more variation in weather and relax concerns about SUTVA violations (e.g., extreme weather in one block-group affecting nearby areas); second, they may introduce bias from geographic sorting – for instance, if wealthier, more Democratic-leaning areas with greater capacity for climate adaptation also experience more extreme weather.

As shown in columns 3 and 4, the estimated effects increase substantially, by factors of 5.6 (temperature) and 3.4 (precipitation). This pattern is consistent with SUTVA violations or suggests that block-group fixed effects absorb important within-district-year variation positively correlated with Democratic vote share. To be conservative, we proceed with specifications including block-group fixed effects, interpreting our estimates as lower bounds.

Columns 5–7 report standard errors adjusted for spatial autocorrelation using the Conley (1999) estimator with radii of 25, 50, and 100 km. The precision of our estimates remains unaffected, reinforcing their robustness.

In Appendix Figure A.11, we explore whether our climate variables affect turnout. It appears that temperature extremes do affect turnout, which may partially explain the effects on vote margins. However, the magnitude is not sufficient to fully account for the observed impact. Notably, extreme precipitation has no statistically significant effect on turnout and when estimating models that controlling for turnout – despite its potential endogeneity – the estimated effects on Democratic vote share remain significant, indicating that turnout does not fully mediate the relationship.

Robustness to Climate Variable Definitions. To test sensitivity to our choice of climate measures, Figure 3 presents estimates using alternative bin-based temperature and precipitation variables. The vote share effects for temperature are clearly concentrated in the extreme ranges, particularly for counts of days above 25°C. Precipitation effects, by contrast, emerge at more moderate levels.

Consistent with these patterns, Appendix Figure A.9 shows binned scatter plots using average (rather than extreme) weather conditions. The results have the same sign as in our baseline specification but are attenuated and less precisely estimated—unsurprising given prior evidence that extreme events, not averages, drive behavioral and economic outcomes (e.g. Schlenker and Roberts (2009) in the case of agriculture and Carleton et al. (2022) in the case of mortality). We therefore focus on extremes in our main analysis.

Appendix Figure A.10 provides evidence that the relationship between extreme weather and Democratic vote margin is not limited to specifications with congressional district $\times$ election fixed effects. A potential concern with our preferred specification is that, by absorbing a large share of the variation through tight fixed effects, it may rely on residual variation that is noisier or less representative. Reassuringly, estimates from a specification that includes only block-group and year fixed effects yield consistent results, with even larger magnitudes. This strengthens confidence in the robustness of our findings. Nonetheless, we proceed with the more conservative specification that includes congressional district $\times$ election fixed effects, as it flexibly accounts for supply-side factors and isolates the demand-side impact of climate extremes.

Appendix Tables A.6 and A.7 further confirm the robustness of our findings across various climate variable specifications—including average versus extreme values, and positive versus negative deviations—with and without block-group fixed effects and controls. All results are qualitatively consistent with our main estimates.

3.2 Incorporating Climate Adaptation: Green and Brown Jobs

We now turn to labor market changes associated with climate policy. Specifically, we investigate how the local shares of green and brown jobs—defined in Section 2—relate to electoral outcomes. Green jobs are those linked to green activities, while brown jobs are tied to oil and gas extraction, coal mining and their support activities. We hypothesize that a higher share of green jobs increases support for climate-friendly policies—such as carbon pricing and green subsidies—and thus boosts the vote share for Democratic candidates, who tend to advocate for such policies during our sample period. Conversely, we expect a higher share of brown jobs to reduce Democratic support.

We extend equation (2) as follows:

$$y_{bt} = \delta^{temp} Temp_{bt} + \delta^{prec} Precip_{bt} + \delta^{brown} ShBrEmp_{bt} + \delta^{green} ShGrEmp_{bt} + \alpha X_{bt} + \mu_b + \Omega_{c(b),t} + \epsilon_{bt} \quad (3)$$

where $ShGrEmp_{bt} = GreenEmp_{bt}/Emp_{bt}$ is the share of green employment $GreenEmp_{bt}$ as described in Section 2 and total employment Emp_{bt} in block-group b (from LODES RAC). The share of brown jobs $ShBrEmp_{bt}$ is defined analogously.

Identifying the causal effect of green and brown jobs on vote margins poses a distinct set of challenges relative to our climate variables. First, there is less within–block-group variation over time in employment composition than in weather shocks, as employment profiles tend to persist across congressional cycles. Nevertheless, due to the high spatial granularity of our voting data, we are still able to detect meaningful effects from the substantial job shifts that do occur. We therefore include green and brown employment terms alongside weather variables in equation (3), allowing us to directly compare their estimated effects.

A second challenge is potential endogeneity. As with climate exposure, omitted variable bias can arise if unobserved characteristics influence both employment composition and voting behavior. For instance, block-groups with higher brown job shares may inherently lean more conservative, regardless of employment, due to broader regional or cultural factors. Furthermore, green and brown jobs are not randomly distributed: green subsidies may be targeted to either politically contested areas or partisan strongholds, introducing ambiguity in the expected direction of bias. To address this, we adopt an instrumental variables strategy, constructing shift-share instruments based on national trends in green and brown employment (the "shift") and initial year 2000 local employment shares (the "share"), as detailed in Appendix Section B.3. Following Borusyak, Hull and Jaravel (2022), we control for initial employment shares whenever block-group fixed effects are excluded.

Table 2 presents estimates from several variants of equation (3). Columns 1-3 include block-group and congressional district $\times$ election year fixed effects. Column 2 adds media market (DMA) $\times$ election year fixed effects to account for media-driven variation in climate salience. Column 3 also adjusts standard errors for spatial autocorrelation using a 100 km radius.

As expected, a higher share of brown employment is associated with lower Democratic vote margins. The effect is substantial: a one standard deviation increase in brown job share (1.75 percentage points) reduces the Democratic margin by 0.62 percentage points (Column 1). For green employment, we find a positive association with

Democratic support, albeit smaller in magnitude. A one standard deviation increase in green job share (0.62 percentage points) raises the Democratic vote margin by 0.21 percentage points. Including DMA $\times$ election year fixed effects in Column 2 does not materially alter these results. Moreover, comparing Table 2 to Table 1, we observe that controlling for the effects of jobs does not meaningfully affect the estimated impacts of climate shocks.

Columns 4 and 5 report estimates omitting block-group fixed effects. As we saw in Table 1, our estimated coefficients increase in absolute magnitude. However, while the effect of brown jobs remains negative, the green jobs coefficient turns negative as well, contrary to our hypothesis. This reversal may be due to green employment being correlated with unobserved block-group characteristics that correlate positively with Republican vote share. Indeed, green job shares are, in fact, positively correlated with control variables such as the share of married individuals or rural residents, and negatively correlated with the share of college-educated residents. These patterns suggest that green employment is likely confounded with unobserved block-group characteristics not fully captured by our control set. This provides additional support for including block-group fixed effects, even at the cost of reduced variation in demand factors.

Columns 6 and 7 present IV estimates using our shift-share instruments. Column 6 includes block-group fixed effects, while Column 7 omits them. The IV estimates largely confirm our OLS findings, particularly regarding brown jobs. However, the estimated effect of green employment increases notably, suggesting attenuation bias in the OLS estimates, likely due to measurement error. This is plausible, as green employment is often dispersed across emerging or ambiguously classified sectors, unlike brown jobs, which are concentrated in well-defined fossil fuel industries.

Overall, our demand-side analysis yields several key insights. First, concerns that weak voter demand might explain limited climate policy action appear unfounded. Local temperature and precipitation shocks significantly shift political behavior—consistent with models of learning or salience, as in Hoffmann et al. (2022). Second, local labor market changes also matter, though their estimated effects are somewhat less stable and precise than those of weather shocks. In line with expectations, green jobs predict greater support for Democratic candidates, while brown jobs predict the opposite.

In terms of explanatory power, employment shocks and climate shocks are roughly comparable in magnitude. A one standard deviation increase in extreme temperature or precipitation has a similar effect on Democratic vote share as a comparable change in green or brown job shares. In sum, both climate-related weather shocks and mitigation-related employment exert quantitatively meaningful and directionally

consistent influence on voter demand for climate policy.

3.2.1 Further Demand Robustness: Evidence from Elections of Energy Regulators

The analysis of demand so far was designed to concentrate on the elements of voter choice specifically relevant for the election of environmentally responsive candidates in U.S. congressional races. Nonetheless, during congressional campaigns a large number of policy issues are typically debated and party identifiers operate as proxies of much more than environmental policy alone. An assessment of contamination due to other correlated policy dimensions –different from the environmental one– and pure partisan divisions is necessary.

An ideal robustness test along these lines would involve a check of whether our approach to demand provides consistent estimates of demand sensitivities to weather and employment shocks also when applied to electoral races exclusively focused on environmental policy. Furthermore, estimated demand parameters should be have consistent sign and comparable magnitude across congressional elections and exclusively environmentally focused races. While State legislatures or local elections do not focus on unidimensional platforms and are therefore not useful for this contrast, certain state regulators endowed with specific environmental mandates are elected, and not appointed, and these races provide a valid benchmark for robustness. We focus on partisan Railroad Commissioner elections in Texas, building on the idea first proposed in Boomhower (2024), and we estimate our demand specification in this sample.

The Texas Railroad Commission oversees the oil and gas industry, along with natural gas utilities, pipelines, and coal and uranium mining. Its three commissioners are elected on a staggered schedule, with one seat up for election every even-numbered year. We compile precinct-level data on vote shares in these races. Unlike U.S. House elections, where the salience of climate issues may vary depending on candidate platforms, Railroad Commission elections directly concern the regulation of fossil fuel and extractive industries with major environmental implications and without ambiguity.

Appendix Table A.9 reproduces our main specification from Table 2, restricting the sample to Texas and estimating the model separately for U.S. House and Railroad Commission elections. In column 2, we find that the Texas-specific coefficients are quantitatively similar when the outcome is block-group level support for energy regulators. Because Railroad Commissioners focus almost exclusively on energy and environmental regulation, this consistency strengthens the interpretation that our shocks capture demand for climate policy rather than broader partisan alignment. Quantitatively, the

effect of our temperature shock is quite similar between what found for House elections and Railroad Commissioners, while the effect of our precipitation shock is much larger, and significant, for the Railroad Commissioners (perhaps reflecting agricultural interests in water). The brown jobs effect is also slightly larger in magnitude, while the green jobs measure is about the double the size and significant.

In columns 3 and 4, we further include vote shares in the relevant up- or down-ballot race (i.e., U.S. House vote share when the outcome is Commissioner support, and vice versa) as controls. While these controls are endogenous, they provide an important check on whether the effects we estimate are primarily driven by underlying partisanship. We find that three of the four shocks are insignificant in U.S. House elections when controlling for Commissioner vote shares, but all four are significant in Commissioner races when controlling for House vote shares. This asymmetry suggests that the shocks affect voting behavior in climate salient elections in ways not fully explained by partisanship alone.

3.3 Demand Heterogeneity

To conclude our demand analysis, we also examine the heterogeneity implied by models of political competition (Persson and Tabellini, 2002). If climate shocks push voters towards wanting more left-wing climate policy, the effects of demand shocks on Democratic vote margins should be larger when the difference in the candidate climate ideal points is larger, as the voters will be more attracted to the Democrats than the Republicans. We show this formally in Appendix C.

As the ideal points of candidates are endogenous, we leverage the same variables we use as instruments in the supply analysis below: the average climate ideal point of candidates from the same party in neighboring districts. We then calculate the difference between the two candidates in this measure for each Congressional race. Appendix Figure A.14a and Appendix Figure A.14b both show that the climate effects are larger where the difference in neighboring same-party candidate ideal points is larger. In Appendix Table A.8 we further show that the effects of *all* of our demand shocks are larger when the Republican and Democratic candidates are farther apart in (the exogenous component of) climate ideology, either measured averaging over all years, or measured using only contemporaneously measured ideology. This heterogeneity provides additional evidence that climate shocks are changing vote margins by changing voters' preferences for climate policy towards the platforms of Democrats.

In principle, these and other sources of heterogeneity could be incorporated into the structural analysis and projections below. However, we focus on our simpler, linear

model of demand in order to retain enough precision to make meaningful forecasts out to 2050.

4 Estimating Effects on Politician Supply

This section extends our empirical analysis beyond voter demand. The reasons for focusing on political supply in the context of climate politics are twofold. First, by focusing on the demand-supply equilibrium, we are able to recover important parameters, such as the sensitivity of platforms to expected vote shares and the sensitivity of vote shares to changes in the policy platforms of politicians. Second, a full system for demand and supply is necessary for forecasting future political equilibria and performing the projections in Section 5.

The reduced-form estimates in the previous section are internally valid estimates of the effects of climate changes and climate-related employment changes on partisan vote shares, holding fixed candidates and campaign platforms in each U.S. House election. Given our interest in predicting the effect of climate change on equilibrium policy, however, we need to account for the sensitivity of policy platforms to expected vote shares. We also need to account for how shocks change the supply of environmental policies, as temperature, precipitation, and employment could directly affect candidate ideal points on climate, independently of effects on voter demand.

Estimating these effects means leaving the within-congressional district×election year variation and moving to cross variation, as candidate platforms only vary across congressional races. Our demand estimates in Section 3 still help identify policy supply by capturing voters' reactions to the shocks. They therefore allow us to recover the shocks' direct effects on supply while accounting for the indirect effects that operate through changes in political demand.

In this section, we work with an empirical model for integrating political demand and supply for our problem. As a simple microfoundation for our system of equations, we set up and solve a standard probabilistic voting model of political competition over climate policy in Appendix C. The model illustrates why conditioning on equilibrium supply platforms is important for recovering demand, and why controlling for demand parameters is important for recovering the direct effects on supply. We deliberately keep our structural framework streamlined (i.e. linear in the parameters) rather than adopting the full set of functional forms implied by the underlying voting model. This choice enhances the transparency of identification. The model's parametric simplicity also improves statistical precision and facilitates out-of-sample forecasting of politi-

cal equilibria under climate change, as we demonstrate in Section 5. More complex structures would complicate forward-looking simulations and require additional data that may be unavailable. Despite its simplicity, our framework captures meaningful and non-obvious interactions between demand and supply in response to climate and employment shocks.

4.1 Supply Specification

As political competition occurs at the congressional district level c in election year t and policy platforms of Republicans, x^r_{ct}, and Democrats, x^d_{ct}, vary only across districts, we cannot rely solely on our block-group level b variation.

Denote by B_c the set of all block-groups in congressional district c. Maintaining the definition of y_{bt} as the block-group level winning margin of the Democrat at time t, denote $\bar{y}_{ct}$ the average winning margin of the Democratic candidate in district c. Further indicate with $\mathbf{V}_{bt}$ block-group exogenous determinants including weather shifters, employment (including green and brown jobs), and other exogenous covariates, such as the employment rate, and with $\bar{\mathbf{V}}_{ct}$ the vector of averages of these covariates in congressional district c at time t.

We model a candidate's policy position as a function of four components. First, a set of exogenous determinants, $\bar{\mathbf{V}}ct$, captures changes in candidate preferences driven by district conditions and candidate learning. Second, candidate positions respond to expected electoral support, proxied by $\bar{y}_{ct}$. Third, we include district and election-year fixed effects, along with an idiosyncratic error term, to account for unobserved heterogeneity. Fourth, we incorporate a party-specific supply shifter, z^p_{ct}, which reflects broader party p effects and non-local factors affecting the candidate's platform choice. We define z^d_{ct} for Democratic Party candidates as the average of the environmental policy positions taken by other Democrats in congressional districts immediately neighboring c within the state. Similarly, z^r_{ct} is defined for Republican Party candidates. We assume that each party's supply shifter only affects that party candidate's supply (conditional on district and election year fixed effects), and is orthogonal to other, unobserved determinants of policy supply and demand. Democrat supply of policy x^d_{ct} is only a function of z^d_{ct}, and similarly for the Republican candidate (these, however, depend on each other through their effects on expected vote shares). These supply shifters not only enhance realism by allowing local party effects to influence candidate platforms, but they are also crucial for identification. Without z^p_{ct}, our empirical model would lack the necessary exogenous variation to isolate the effects of changes in policy platforms and other endogenous variables on vote shares. Finally, z^p_{ct} can be calculated

forward for the 2022-2050 projections, an essential feature necessary for the analysis of Section 5.

With these elements in mind, we can write Democrat policy supply as:

$$x_{ct}^{d} = \lambda^{d}\bar{\mathbf{V}}_{ct} + \beta^{d}\bar{y}_{ct} + \pi^{d}z_{ct}^{d} + \omega_{c}^{d} + \zeta_{t}^{d} + \eta_{ct}^{d}, \tag{4}$$

and, similarly, the Republican policy supply function is given by:

$$x_{ct}^{r} = \lambda^{r}\bar{\mathbf{V}}_{ct} + \beta^{r}\bar{y}_{ct} + \pi^{r}z_{ct}^{r} + \omega_{c}^{r} + \zeta_{t}^{r} + \eta_{ct}^{r}. \tag{5}$$

To close the empirical model, let us recall our demand specification from Section 3:

$$y_{bt} = \delta\mathbf{V}_{bt} + \Omega_{ct} + \mu_{b} + \varepsilon_{bt}. \tag{6}$$

It is important here to notice that we can consistently estimate the coefficient vector δ using the approach of Section 3. To further capture cross-district variation in demand driven by candidate positions, we parameterize the district-by-year fixed effects Ω_{ct} as:

$$\Omega_{ct} = \gamma^{d}x_{ct}^{d} + \gamma^{r}x_{ct}^{r} + \mu_{c} + \kappa_{t} + \varepsilon_{ct}. \tag{7}$$

This specification allows the average democratic vote share in a district-year, net of block-group fixed effects and block-group time-varying covariates $\mathbf{V}_{bt}$, to be driven by Democratic and Republican campaign platform positions. Combining equations (6) and (7) and aggregating at the (c,t) level, we have the demand function:

$$\bar{y}_{ct} = \delta\bar{\mathbf{V}}_{ct} + \gamma^{d}x_{ct}^{d} + \gamma^{r}x_{ct}^{r} + \underbrace{(\mu_{c} + \bar{\mu_{c}})}_{\nu_{c}} + \kappa_{t} + \underbrace{(\varepsilon_{ct} + \bar{\varepsilon}_{ct})}_{\xi_{ct}} \tag{8}$$

where $\bar{\cdot}$ denote district averages of the block-group level variables.

Our empirical model therefore consists of the set of equations (4), (5), and (8), which jointly describe the congressional race political equilibrium. The system (4), (5), and (8) is statistically identified and a constructive proof is offered in Appendix D.

4.2 Estimation

We estimate the system of equations using a two-step GMM procedure. The first step involves a block-group level demand estimation, which we have already performed in Section 3. We employ equation (6) to estimate $\hat{\delta}$ and district-by-year fixed effects $\hat{\Omega}_{ct}$. The second step proceeds by performing the district-level estimation. Starting

from equations (4), (5), and (7), we can substitute in the estimated district-by-year fixed effects $\hat{\Omega}_{ct}$ and employ a (weighted) two-step Generalized Method of Moments (GMM) to estimate all remaining parameters.

Specifically, we first apply the Frisch-Waugh-Lovell theorem to partial out the congressional district fixed effects and year fixed effects from $\bar{\mathbf{V}}_{ct}$, z^d_{ct}, z^r_{ct}, x^d_{ct}, x^r_{ct}, $\bar{y}_{ct}$, and $\hat{\Omega}_{ct}$, and obtain $\tilde{\bar{\mathbf{V}}}_{ct}$, $\tilde{z}^d_{ct}$, $\tilde{z}^r_{ct}$, $\tilde{x}^d_{ct}$, $\tilde{x}^r_{ct}$, $\tilde{\bar{y}}_{ct}$, and $\tilde{\Omega}_{ct}$. Denoting $\tilde{\eta}^d_{ct} = \tilde{x}^d_{ct} - \left(\lambda^d \tilde{\bar{\mathbf{V}}}_{ct} + \beta^d \tilde{\bar{y}}_{ct} + \pi^d \tilde{z}^d_{ct}\right)$, $\tilde{\eta}^r_{ct} = \tilde{x}^r_{ct} - \left(\lambda^r \tilde{\bar{\mathbf{V}}}_{ct} + \beta^r \tilde{\bar{y}}_{ct} + \pi^r \tilde{z}^r_{ct}\right)$, and $\tilde{\varepsilon}_{ct} = \tilde{\Omega}_{ct} - \gamma^d \tilde{x}^d_{ct} - \gamma^r \tilde{x}^r_{ct}$, our sample moment conditions are:

$$
\begin{aligned}
\tilde{\eta}^d_{ct} \cdot \left[\tilde{\bar{\mathbf{V}}}'_{ct}, \tilde{z}^d_{ct}, \tilde{z}^r_{ct}\right] &= \mathbf{0}, \\
\tilde{\eta}^r_{ct} \cdot \left[\tilde{\bar{\mathbf{V}}}'_{ct}, \tilde{z}^d_{ct}, \tilde{z}^r_{ct}\right] &= \mathbf{0}, \\
\tilde{\varepsilon}_{ct} \cdot \left[\tilde{z}^d_{ct}, \tilde{z}^r_{ct}\right] &= \mathbf{0}, \\
\text{Cov}(\tilde{\eta}^d_{ct}, \tilde{\eta}^r_{ct}) &= 0, \\
\text{Cov}(\tilde{\varepsilon}_{ct}, \tilde{\eta}^r_{ct}) &= 0, \\
\text{Cov}(\tilde{\eta}^d_{ct}, \tilde{\varepsilon}_{ct}) &= 0,
\end{aligned}
$$

In order to correct for the fact that the demand district-by-year fixed effects, $\hat{\Omega}_{ct}$, which are outcomes in equation (7), are estimated and are therefore affected by sampling error, we weight each (c,t) observation by the inverse of the variance of the estimated $\hat{\Omega}_{ct}$ in the GMM objective function.

For the computation of the asymptotic variance-covariance matrix of the GMM estimator, we use a degrees of freedom correction based on the number of equations in the system and cluster our standard errors at the congressional district level.

4.3 Results of the Equilibrium Model

Table 3 presents the estimates of our equilibrium model. The table is divided into three parts, corresponding to the system of equations (4), (5), and (8). The first part of the table reports estimates for the position of the environmental policy platform of the Democrats, based on equation (4). A one standard deviation increase in the number of days with temperature exceeding two standard deviations results in Democrats shifting their environmental policy position to the right by 0.016 (=0.002 $\times$ 8.13) points, equivalent to 5% of the sample standard deviation in Democratic positions. The effect of precipitation on Democratic positioning is negligible.

Temperature making Democratic candidates more moderate may seem counterintuitive. However, it is important to note that this effect is *net* of the effect on voter demand, and so can be interpreted as the additional effect of climate on the candidate's ideal point. Thus, candidates are not pulled to the left in climate *as much* as would be predicted by demand alone. This could be because of a variety of forces (e.g., candidate selection, special interests influence, etc.), or simply any unmodeled mechanism where climate shocks make future climate policy more salient, and so candidates decide to pivot to the center to compete more effectively on this dimension.

While imprecisely estimated, the effects of green and brown jobs on Democratic positioning are similar in magnitude, but intuitively opposite in direction. For instance, a one standard deviation increase in brown jobs moves Democrats 0.034 points closer to the center, whereas a comparable increase in green jobs shifts their position 0.043 points further to the left.

Democrats are also highly responsive to changes in expected voter demand. A one standard deviation increase in their expected vote share difference allows Democratic party candidates to shift 0.63 points further to the left in the policy space, equivalent to almost a two-standard-deviation shift. Furthermore, the coefficient on the supply shifter z^d_{ct} is statistically significant, indicating that Democrats, intuitively, adjust their positions based on the environmental policies of their local congressional delegation. This also indicates a strong first-stage for identifying the Democratic supply equation. The estimated slope is 0.18, however, an effect well below a 1:1 pass-through of party policy onto candidates' positions. We interpret this magnitude as indicating that party influence on environmental platforms, while present, is not overwhelming.[10]

The second part of Table 3 reports estimates for the Republicans' environmental policy positioning, based on equation (5). In contrast to Democrats, Republican candidates are generally less responsive to weather and job shocks. Republicans' policy positions are, however, significantly dependent on the expected vote share advantage of Democrats. The marginal effect of β^r is less than one-fifth that of the corresponding Democratic marginal effect and has the opposite sign: a one standard deviation increase in Democratic vote share leads Republican candidates to adopt a more conservative policy stance. This may reflect a strategy of reinforcing conservative credentials or signaling "character" in the sense of Kartik and McAfee (2007). Within the framework

[10] An interesting contrast here is between the pre-electoral party influence estimated in this model and the much higher post-electoral party influence estimated in post-electoral models, such as Canen, Kendall and Trebbi (2020) and Canen, Kendall and Trebbi (2021). It seems plausible that parties may allow more flexibility at a time when the key concern is getting their own representatives elected, relative to the point where the legislative party line needs to be voted and passed.

of Appendix C this pattern could arise when Republican candidates either (i) judge their chances of winning to be slim, prompting them to signal their true ideological stance to voters or party leaders, or (ii) place greater weight on policy goals than on electoral victory.

In the last part of the panel, we see that the party shifter z^r_{ct}'s slope is statistically significant. Similarly to Democrats, the estimated coefficient is around 0.2 and statistically different from 1. This finding suggests that, even within the Republican Party, local party delegations do not fully determine candidates' platform choices. Instead, candidates retain substantial discretion in shaping their local environmental positions. This is particularly noteworthy given the common assumption that platforms have become increasingly "nationalized" in recent years, as argued by Hopkins (2018).

The final part of Table 3 provides estimates for the district-level demand equation (equation (8)). By construction, the effects of weather and job shocks on voter demand are the same as those observed in Section 3. What the district-level demand equation reveals is that voters are significantly more responsive to shifts in Democratic platform positioning compared to Republican positioning. For example, holding the environmental position of the Republican candidate constant, a move of one standard deviation to the right (i.e. towards the center) by a Democratic candidate increases their vote margin by 9.2 percentage points. In contrast, a one standard deviation move to the right by Republican candidates decreases the Democratic vote margin by only 0.59 percentage points.

In Appendix Table A.10, we re-estimate the model, incorporating controls for differences in employment, income, and voting-age population at the congressional district level, added symmetrically to all three equations of the system. The results confirm that our estimates remain robust when accounting for these additional district characteristics.

As an additional check on our supply estimation, we conduct a placebo exercise where we re-estimate the model, but use only the *cultural* ideal points of the candidates, excluding the environmental dimension.[11] Appendix Table A.11 shows the resulting estimates. Naturally, the response of voter demand to our climate and job shocks remain unchanged, as these are estimated using within-district-year variation. However, we also see that none of these shocks affect candidate cultural ideal points. Furthermore, the cultural ideal points do not affect overall voter demand, and these remain identified because the instruments (neighboring same-party cultural ideal points) are still relevant. This exercise shows that our environmental ideal points reflect not

[11] Longuet-Marx (2024) shows that Democrats treat environmental issues as cultural, while Republicans treat them as economic issues.

just general ideological positions, but a specific, climate-relevant dimension.

Reduced-form Estimates. Given our structural estimates, one can calculate reduced-form coefficients, providing insight into how the model's exogenous variables (e.g., weather shocks, employment, party supply shifters) influence equilibrium supply and demand responses.

Specifically, define $\Xi = \dfrac{1}{1-\beta^d\gamma^d-\beta^r\gamma^r}$, $\Lambda_{ct} = \xi_{ct} + \gamma^d\eta^d_{ct} + \gamma^r\eta^r_{ct}$, $\alpha_{ct} = \nu_c + \kappa_t$, $\rho^d_{ct} = \omega^d_c + \zeta^d_t$, and $\rho^r_{ct} = \omega^r_c + \zeta^r_t$. Then, the reduced-form equations for the demand and supply system are:

$$
\begin{aligned}
\bar{y}_{ct} =& \Xi\left(\alpha_{ct} + \gamma^d\rho^d_{ct} + \gamma^r\rho^r_{ct}\right) + \Xi\left(\tilde{\delta} + \underline{\gamma^d\lambda^d + \gamma^r\lambda^r}\right)\bar{\mathbf{V}}_{ct} \\
&+ \left(\Xi\gamma^d\pi^d\right) z^d_{ct} + \left(\Xi\gamma^r\pi^r\right) z^r_{ct} + \left(\Xi\Lambda_{ct}\right) \\
x^d_{ct} =& \left(\rho^d_{ct} + \beta^d\Xi\left(\alpha_{ct} + \gamma^d\rho^d_{ct} + \gamma^r\rho^r_{ct}\right)\right) + \left(\tilde{\lambda^d} + \underline{\beta^d\Xi\left(\delta + \gamma^d\lambda^d + \gamma^r\lambda^r\right)}\right)\bar{\mathbf{V}}_{ct} \\
&+ \left(\beta^d\Xi\gamma^d\pi^d + \pi^d\right) z^d_{ct} + \beta^d\left(\Xi\gamma^r\pi^r\right) z^r_{ct} + \left(\beta^d\Xi\Lambda_{ct} + \eta^d_{ct}\right) \\
x^r_{ct} =& \left(\rho^r_{ct} + \beta^r\Xi\left(\alpha_{ct} + \gamma^d\rho^d_{ct} + \gamma^r\rho^r_{ct}\right)\right) + \left(\tilde{\lambda^r} + \underline{\beta^r\Xi\left(\delta + \gamma^d\lambda^d + \gamma^r\lambda^r\right)}\right)\bar{\mathbf{V}}_{ct} \\
&+ \beta^r\left(\Xi\gamma^d\pi^d\right) z^d_{ct} + \left(\beta^r\Xi\gamma^r\pi^r + \pi^r\right) z^r_{ct} + \left(\beta^r\Xi\Lambda_{ct} + \eta^r_{ct}\right).
\end{aligned}
$$

These coefficients allow us to distinguish between direct effects and indirect effects. To see these effects visually in the system above, we mark with a tilde ($\tilde{\cdot}$) the parameters that reflect the direct effects and underline ($\underline{\cdot}$) the parameters that represent the indirect effects.

The results are presented in Table 4, which is divided into three panels, corresponding to the three estimating equations. The reduced-form coefficients related to weather and job shocks are shown across the rows. In columns (1)–(3), we report the effects of temperature shocks on Democratic vote margin, decomposing the total effects into a direct component (δ_{temp}) and indirect effects arising from changes in policy positions ($\gamma^d\lambda^d + \gamma^r\lambda^r$). As observed in the previous table, temperature shocks are associated with an increase in the share of Democratic votes. Notably, Democrats respond to these shocks by shifting slightly to the right, and even small rightward shifts lead to higher vote margins. Consequently, the indirect effect is positive and comparable in magnitude to the direct effect.

Despite Democrats' tendency to shift rightward in response to temperature shocks, their actual movements in equilibrium are a precise zero (see column 6). This is because

the increase in expected vote margin simultaneously allows them to shift further to the left, as indicated by the β_d coefficient.

Republican responses to temperature shocks are negligible, with small and statistically insignificant effects (see columns 7-9). Similarly, the effects of precipitation largely align with those of temperature shocks, though they are smaller in magnitude and statistically imprecise.

The last two rows of the table present the reduced-form effects of brown and green jobs. As observed in the demand-side estimation, a higher share of brown jobs is negatively associated with Democratic vote margin. However, in equilibrium, these effects are muted as Democrats adopt more conservative environmental positions. The resulting shift is sufficiently large that the total effect becomes positive, although it is not statistically significant (see column 6).

In contrast, the effects of green jobs are more pronounced. As seen in the demand-side estimation, a higher share of green jobs is positively associated with Democratic vote margin. However, two supply-side factors offset this effect. First, as the share of green jobs increases, Democratic candidates shift their platforms further to the left. Second, as their vote margin increases, they move even further leftward (column 6). The combined effects of these two forces result in a total effect that, although imprecisely measured, is negatively associated with Democratic vote margin. A rationalization of this finding is plausible. It would appear as Democratic candidates, who may be uncertain about the exact elasticity of vote margins to green jobs, overestimate the the support they may garner from green transition employment, especially in terms of how extreme a policy position green jobs may afford them in the campaign.

5 Projecting Political Impacts of Climate Change

The results of the econometric model so far present a series of economically relevant political elasticities, yet they do not make immediately explicit how climate shocks and employment changes may ultimately translate into different political equilibria in the future. For example, it is unclear based on Table 3 alone how big of a difference medium-term weather shocks to a solid Democratic state like California rather than weather shocks to a swing Republican leaning state like Arizona may matter electorally, and in terms of House majorities and roll-call voting.

Indeed, climate shocks to California may lead to no major congressional composition change, leaving Democratic seat shares unchanged in the future. Temperature and precipitation shocks in Arizona may erode substantially Republican seat shares, shifting

support to more climate friendly politicians.

Using the projected values of our independent variables discussed in Section 2, we obtain location-specific estimates for every election year from 2022 to 2050.

We use the model's reduced-form coefficients to project how the political equilibrium will evolve over time in response to climate and employment changes until the year 2050. To do so, we begin the projections in 2022, using each congressional district's observed baseline values for (i) the Democrat's vote margin $\bar{y}_{ct}$, (ii) the Democrat's policy position x^d_{ct}, and (iii) the Republican's policy position x^r_{ct}. At two-year intervals (i.e., 2022, 2024, 2026, etc.), we construct the policy shifters z^d_{ct} and z^r_{ct} by taking the average of the lagged x^d and x^r from adjacent districts of district c. We then incorporate the predicted district-level weather shocks (temperature and precipitation extremes), obtained from multiple climate models, as well as predicted green and brown employment rates, and updated policy shifters into the reduced-form expressions to calculate the next-period values for $\bar{y}$, x^d, and x^r. In each projection step, we fix the district- and year-specific fixed effects (estimated from the structural estimation) to their 2020 values, thus assuming no redistricting and no further unobserved shocks beyond those captured by weather and employment. The updated outcomes, $\left(\bar{y}_{c,t+2}, x^d_{c,t+2}, x^r_{c,t+2}\right)$, then serve as initial conditions for the subsequent congressional cycle. Iterating this process through 2050 provides a forward simulation of each district's vote margin and policy positions under evolving weather and employment structures, while holding the unobserved district and year-specific components at their baseline levels.

To construct 95% confidence intervals, we perform a 5,000-round bootstrap. In each round, we draw the structural coefficients from a multivariate normal distribution with means equal to the estimated parameters and a covariance matrix given by the cluster-robust variance estimates from the two-step GMM. We also randomly sample residuals from the structural estimation and add them to the predicted $\bar{y}_{ct}$, x^d_{ct}, and x^r_{ct}. This procedure produces predictive intervals that account for both parameter uncertainty and unexplained variation in the original estimates.

In Panel A of Figure 4, we plot the contribution of temperature shocks to Democratic vote margins, averaged across congressional districts from 2022 to 2050, under two different temperature scenarios: SSP5-8.5 and SSP1.2-6. The SSP5-8.5 scenario assumes that carbon emissions continue to increase along historical trends without policy mitigation, while the SSP1-2.6 scenario reflects the highest level of climate change mitigation, keeping global surface temperature changes below 2 degrees Celsius. For these reasons, the two scenarios can be interpreted as conceptual upper (pessimistic) and lower (optimistic) bounds in this exercise. Figure 4 also decomposes the effects into temperature's direct impact on vote margins and the indirect effects generated by

Democratic and Republican policy responses. The final plot in each panel presents the total effects.

Under the SSP5-8.5 scenario, we project average Democratic vote margins to increase by 1.4 percentage points by 2050. This increase arises both from the direct effects of rising temperature shocks on vote margin and the indirect effects of Democratic candidates shifting slightly to the right, a response that resonates strongly with voters. As expected, the effects are more muted under the SSP1-2.6 scenario, where Democratic vote margins are projected to increase by 0.8 percentage points.

In Panel B, we present the contribution of precipitation shocks to projected vote margins under the two climate scenarios. Unlike temperature shocks, the effects of precipitation are statistically imprecise, as suggested by our reduced-form estimates. Both climate models indicate that the impact of precipitation on vote margins will change about 0.2 percentage point over the projection period.

Panel C displays projections for the effects of employment shifts in green and brown jobs on Democratic vote margins, using the BLS OOH projections. Because these projections anticipate only a slight rise in the green-job share and an equally modest decline in the brown-job share, we expect the resulting electoral and ideological effects to be correspondingly small.[12] As observed in Table 4, an increasing share of green jobs in a district is associated with greater support for Democratic candidates. However, this support is unlikely to grow over time. Democrats respond to this increased support by adopting more liberal environmental platforms, leading to a total effect on vote shares that remains negative throughout the period. This correction should not be overinterpreted, as the effect is not statistically precise.

The contribution of brown jobs to Democratic vote margins follows a similar, albeit opposite, trend. We project the total effects of brown jobs on vote margins to remain positive but small in magnitude and statistically imprecise throughout the projection period. Overall, our projections suggest that mitigation through job composition shifts appear, based on current information, not a major source of political shift for the period 2022-2050.

Spatial Heterogeneity The results in Figure 4 are averaged across all congressional districts and therefore mask substantial variation across states. To unpack this heterogeneity, Figure 5 shows, for each district, the change between 2022 and 2050 in how projected shifts in exogenous variables affect candidates' ideological positions, the

[12] These moderate expected changes in employment may stem from the expectation that these sectors will change little between 2023 and 2033 but could follow a different trajectory from 2033 to 2050. Because we simply extend the 2023–2033 trend through 2050, we may under-estimate the magnitude of future changes.

Democratic vote margin, and the likely winning party. Appendix Figure A.19 breaks these differences down by state, and Appendix Figure A.20 presents the same information on a hexagonal cartogram that highlights the congressional district distribution by state.

Panels A and B reveal a clear convergence in the U.S. South: Republicans grow somewhat more progressive, while Democratic candidates become more conservative on environmental issues. Panel C then illustrates the impact of all shocks on the projected Democratic vote margin in each district. Every district shows a positive effect for the Democratic Party, though its magnitude varies widely across space.

The largest temperature shocks are predicted to occur in the Southwest—Oklahoma, Colorado, Texas, and Arizona—where days exceeding two standard deviations rise by an average of 68 under the SSP5-8.5 scenario. We estimate this increase boosts Democratic vote margins by roughly 3 percentage points in these states by 2050. In contrast, Massachusetts, Illinois, and Rhode Island see gains of less than 1 percentage point. Furthermore, Democratic moderation on environmental issues in parts of the Southeast drives significant vote swings in Alabama, Georgia, and Florida. Finally, Panel D maps the projected 2050 electoral outcome: compared to 2022, Democrats pick up four additional seats, two of which are in the South. Endogenous demand and supply responses in the model somewhat limit the extent of more substantial party switching.

Compositional Changes to the House of Representatives Given our projected effects on vote share, one might wonder whether these changes are sufficiently large to substantively alter the composition of the House of Representatives and potentially its ideological orientation. In Figure 6, we present four plots, all corresponding to the SSP5-8.5 scenario. The upper-left quadrant shows the projected share of Democrats elected to the House of Representatives, while the upper-right quadrant depicts both the average and median projected campaign positions on environmental policies of all elected House members. The bottom panels focus on party-specific trends, with the bottom-left plot showing the average and median projected campaign positions among elected Democrats, and the bottom-right plot showing the same for elected Republicans.

Taken as a whole, the plots reveal a changing political landscape. By 2050, the median member of the House, and to a lesser extent the average member, is projected to adopt a more liberal stance on environmental policies compared to 2020. This shift occurs despite the fact that the average and median campaign positions of both elected Democrats and Republicans are becoming more conservative over time. These seemingly contradictory patterns are explained by the increasing share of House seats held

by Democrats, who, while becoming more moderate themselves, remain significantly more liberal on environmental policies compared to their Republican counterparts.

Although these results reflect campaign positions on environmental policies, as demonstrated in Section 4, these ideal points strongly correlate (0.86) with elected members' actual policy positions based on roll-call voting, ultimately reflected in equilibrium policy choices. To gauge the policy impact, we use our estimates to derive counterfactual voting behavior—and thus the probability that Congress enacts climate legislation. The American Clean Energy and Security Act of 2009 ("Waxman–Markey") serves as our benchmark for a carbon-pricing vote. Our roll-call estimates place the median House member in that session (a Democrat) at an environmental ideal point of 0.38, and a predicted probability of voting yes on Waxman-Markey of 63%. Our forecast implies that the median House member's ideology in 2050 will become 0.11 units more progressive, equivalent to shifting their roll-call ideal point to -0.48 and raising the probability of voting yes on emissions pricing to 72%. In other words, the forces in our model raise the probability that the House will pass a carbon-pricing bill by roughly 9 percentage points in 2050 relative to 2020.

6 Conclusion

This paper focuses on the politics of climate in the United States from an empirical perspective. Our main contribution is to econometrically decouple electoral demand drivers from supply drivers of candidate policy platform choices. Within the set of demand forces, we are able to separate effects due to extreme temperature and precipitation from economic drivers, such as the loss of brown jobs and the gain of green jobs in certain geographic areas, which speak to issues of adjustment and adaptation. High temperature shocks and high precipitation shocks increase support for Democrats, and similarly the arrival of green jobs. Brown job gains increase support for Republicans. Both sets of demand shifters have similar economic and statistical significance. On the supply side, Democrats appear more responsive to voter demand for climate policy. In turn, voters are sensitive to the environmental policy choices of Democratic candidates competing in their congressional races, but not of Republicans. Both Democratic and Republican candidates respond to local party effects in their platform decisions, but much less than 100 percent.

We use the parameter estimates from our demand and supply model to project the effects of climate and employment compositional trends 25 years into the future. Under our climate change scenarios, the analysis shows a consistent electoral shift

toward more pro-environmental candidates (Democrats), even as both Democrats and Republicans endogenously become mildly less pro-environment.

Methodologically, we present one of the first structural supply-and-demand equilibrium models of electoral political competition. Demand identification leverages the unique granularity of the data used in this paper, isolating within-district variation to estimate demand, and controlling for demand in recovering supply of candidate policies, measured by ideal points of campaigns. We believe that these ingredients will be important for future, arguably richer and more realistic, quantitative models of electoral competition in political economy beyond the specific topic of climate politics.

Climate change, however, appears set to be a major social cost for the foreseeable future. Adaptation to and mitigation of climate change are going to involve policy decisions that aggregate diverse interests and perspectives. Whether democratic institutions and electoral competition can deliver these policies remains an open question, one that our paper does not forcefully answer in the affirmative. Our model is deliberately streamlined, however, and future work should incorporate other realistic margins of climate change and adaptation (e.g. disasters and migration, as in Desmet and Rossi-Hansberg (2024)), as well as more margins of political influence (e.g. campaign finance and special interest politics).

Finally, a large literature has modeled and measured the unavoidable international cooperation and conflicts over climate policy necessary for adequate mitigation and adaptation (for a recent quantitative macroeconomic example see Bourany (2024)). Rigorously incorporating domestic political economy into these models remains an area for future research.

References

Aklin, Michaël and Johannes Urpelainen. 2013. "Political Competition, Path Dependence, and the Strategy of Sustainable Energy Transitions." *American Journal of Political Science* 57(3):643–658.

Anderson, Soren, Ioana Marinescu and Boris Shor. 2023. "Can Pigou at the polls stop us melting the poles?" *Journal of the Association of Environmental and Resource Economists* 10(4):903–945.

Ansolabehere, Stephen, James M Snyder Jr and Charles Stewart III. 2001. "Candidate positioning in US House elections." *American Journal of Political Science* pp. 136–159.

Autor, David, Anne Beck, David Dorn and Gordon Hanson. 2024. "Help for the Heartland? The Employment and Electoral Effects of the Trump Tariffs in the United States.".
URL: *http://www.nber.org/papers/w32082.pdf*

Bateman, David A, Ira Katznelson and John S Lapinski. 2018. *Southern nation: Congress and white supremacy after reconstruction*. Vol. 158 Princeton University Press.

Bateman, David A and John Lapinski. 2016. "Ideal points and american political development: Beyond dw-nominate." *Studies in American Political Development* 30(2):147–171.

Bergquist, Parrish and Christopher Warshaw. 2019. "Does global warming increase public concern about climate change?" *The Journal of Politics* 81(2):686–691.

Berry, Steve, Christian Cox and Phil Haile. 2024. "What Drives Voting: Estimates from a Multilevel Data." *mimeo Yale* .

Binder, Sarah A. 2004. *Stalemate: Causes and consequences of legislative gridlock*. Rowman & Littlefield.

Bonica, Adam. 2013. "Ideology and interests in the political marketplace." *American Journal of Political Science* 57(2):294–311.

Boomhower, Judson. 2024. "When Do Environmental Externalities Have Electoral Consequences? Evidence from Fracking." *Journal of the Association of Environmental and Resource Economists* 11(4):999–1029.

Borusyak, Kirill, Peter Hull and Xavier Jaravel. 2022. "Quasi-experimental shift-share research designs." *The Review of Economic Studies* 89(1):181–213.

Bourany, Thomas. 2024. "Optimal Energy Policy and the Inequality of Climate Change.".

Burke, Marshall, Mustafa Zahid, Mariana CM Martins, Christopher W Callahan, Richard Lee, Tumenkhusel Avirmed, Sam Heft-Neal, Mathew Kiang, Solomon M Hsiang and David Lobell. 2024. Are We Adapting to Climate Change? Technical report National Bureau of Economic Research.

Burke, Marshall, Mustafa Zahid, Noah Diffenbaugh and Solomon M Hsiang. 2023. Quantifying climate change loss and damage consistent with a social cost of greenhouse gases. Technical report National Bureau of Economic Research.

Béland, Louis-Philippe and Vincent Boucher. 2015. "Polluting Politics." *Economics Letters* 137:176–181.

Calvo, Richard, Vincent Pons and Jesse M Shapiro. 2024. Pitfalls of demographic forecasts of us elections. Technical report National Bureau of Economic Research.

Canen, Nathan, Chad Kendall and Francesco Trebbi. 2020. "Unbundling polarization." *Econometrica* 88(3):1197–1233.

Canen, Nathan J, Chad Kendall and Francesco Trebbi. 2021. Political Parties as Drivers of US Polarization: 1927-2018. Technical report National Bureau of Economic Research.

Carleton, Tamma, Amir Jina, Michael Delgado, Michael Greenstone, Trevor Houser, Solomon Hsiang, Andrew Hultgren, Robert E Kopp, Kelly E McCusker, Ishan Nath et al. 2022. "Valuing the global mortality consequences of climate change accounting for adaptation costs and benefits." *The Quarterly Journal of Economics* 137(4):2037–2105.

Clinton, Joshua, Simon Jackman and Douglas Rivers. 2004. "The statistical analysis of roll call data." *American Political Science Review* 98(2):355–370.

Conley, Timothy G. 1999. "GMM estimation with cross sectional dependence." *Journal of econometrics* 92(1):1–45.

Cox, Christian. 2024. "The Equilibrium Effects of Campaign Finance Deregulation on US Elections." *mimeo University of Arizona* .

Dechezleprêtre, Antoine, Adrien Fabre, Tobias Kruse, Bluebery Planterose, Ana Sanchez Chico and Stefanie Stantcheva. 2022. Fighting climate change: International attitudes toward climate policies. Technical report National Bureau of Economic Research.

Dell, Melissa, Benjamin F Jones and Benjamin A Olken. 2012. "Temperature shocks and economic growth: Evidence from the last half century." *American Economic Journal: Macroeconomics* 4(3):66–95.

Deryugina, Tatyana. 2013. "How do people update? The effects of local weather fluctuations on beliefs about global warming." *Climatic change* 118:397–416.

Desmet, Klaus and Esteban Rossi-Hansberg. 2024. "Climate change economics over time and space." *Annual Review of Economics* 16.

Doyle, Timothy, Doug McEachern and Sherilyn MacGregor. 2015. *Environment and politics*. Routledge.

Eckert, Fabian, Teresa Fort, Peter Schott and Natalie Yang. 2021. "Imputing Missing Values in the US Census Bureau's County Business Patterns.".
URL: *http://www.nber.org/papers/w26632.pdf*

Egan, Patrick J and Megan Mullin. 2012. "Turning personal experience into political attitudes: The effect of local weather on Americans' perceptions about global warming." *The Journal of Politics* 74(3):796–809.

Egan, Patrick J and Megan Mullin. 2017. "Climate change: US public opinion." *Annual Review of Political Science* 20:209–227.

Fredriksson, Per G, Le Wang and Khawaja A Mamun. 2011. "Are politicians office or policy motivated? The case of US governors' environmental policies." *Journal of Environmental Economics and Management* 62(2):241–253.

Gagliarducci, Stefano, M Daniele Paserman and Eleonora Patacchini. 2019. Hurricanes, climate change policies and electoral accountability. Technical report National Bureau of Economic Research.

Gasper, John T and Andrew Reeves. 2011. "Make it rain? Retrospection and the attentive electorate in the context of natural disasters." *American journal of political science* 55(2):340–355.

Geels, Frank W, Frans Berkhout and Detlef P Van Vuuren. 2016. "Bridging analytical approaches for low-carbon transitions." *Nature climate change* 6(6):576–583.

Hahn, Robert W, Nathaniel Hendren, Robert D Metcalfe and Ben Sprung-Keyser. 2024. A welfare analysis of policies impacting climate change. Technical report National Bureau of Economic Research.

Hazlett, Chad and Matto Mildenberger. 2020. "Wildfire exposure increases pro-environment voting within democratic but not republican areas." *American Political Science Review* 114(4):1359–1365.

Healy, Andrew and Neil Malhotra. 2010. "Random events, economic losses, and retrospective voting: Implications for democratic competence." *Quarterly journal of political science* 5(2):193–208.

Hilbig, Hanno and Sascha Riaz. 2024. "Natural disasters and green party support." *The Journal of Politics* 86(1):241–256.

Hoffmann, Roman, Raya Muttarak, Jonas Peisker and Piero Stanig. 2022. "Climate change experiences raise environmental concerns and promote Green voting." *Nature Climate Change* 12(2):148–155.

Hopkins, Daniel J. 2018. *The increasingly United States: How and why American political behavior nationalized*. University of Chicago Press.

Iaryczower, Matias, Sergio Montero and Galileu Kim. 2022. Representation failure. Technical report National Bureau of Economic Research.

Jud, Stefano and Quynh Nguyen. 2024. "Disasters and Divisions: How Partisanship Shapes Policymaker Responses to Climate Change." *Available at SSRN 4870935* .

Kahn, Matthew E and John G Matsusaka. 1997. "Demand for environmental goods: Evidence from voting patterns on California initiatives." *The Journal of Law and Economics* 40(1):137–174.

Kaplan, Ethan, Jörg L Spenkuch and Haishan Yuan. 2019. Natural disasters, moral hazard, and special interests in Congress. In *Moral Hazard, and Special Interests in Congress (September 2019)*.

Kartik, Navin and R Preston McAfee. 2007. "Signaling character in electoral competition." *American Economic Review* 97(3):852–870.

Kuziemko, Ilyana, Nicolas Longuet-Marx and Suresh Naidu. 2023. ""Compensate the Losers?" Economic Policy and Partisan Realignment in the US.".

Lazar, Nomi Claire and Jeremy Wallace. 2025. "Resisting the Authoritarian Temptation." *Journal of Democracy* 36(1):135–150.

List, John A. and Daniel M. Sturm. 2006. "How Elections Matter: Theory and Evidence from Environmental Policy." *The Quarterly Journal of Economics* 121(4):1249–1281.

Longuet-Marx, Nicolas. 2024. "Party Lines or Voter Prefereces? Explaining Political Realignment.".

Manson, Steven, Jonathan Schroeder, David Van Riper, Katherine Knowles, Tracy Kugler, Finn Roberts and Steven Ruggles. 2024. "IPUMS National Historical Geographic Information System: Version 19.0.".
URL: *https://www.nhgis.org/*

Martin, Gregory J and Ali Yurukoglu. 2017. "Bias in cable news: Persuasion and polarization." *American Economic Review* 107(9):2565–2599.

McCarty, Nolan, Keith T Poole and Howard Rosenthal. 2016. *Polarized America: The dance of ideology and unequal riches*. mit Press.

Moore, Frances C, Katherine Lacasse, Katharine J Mach, Yoon Ah Shin, Louis J Gross and Brian Beckage. 2022. "Determinants of emissions pathways in the coupled climate–social system." *Nature* 603(7899):103–111.

Pahontu, Raluca L. 2020. "The democrat disaster: Hurricane exposure, risk aversion and insurance demand." *Risk Aversion and Insurance Demand (January 2020)* .

Persson, Torsten and Guido Tabellini. 2002. *Political economics: explaining economic policy*. MIT press.

Poole, Keith T and Howard L Rosenthal. 2011. *Ideology and congress*. Vol. 1 Transaction Publishers.

Rowan, Sam. 2023. "Extreme weather and climate policy." *Environmental Politics* 32(4):684–707.

Schlenker, Wolfram and Michael J Roberts. 2009. "Nonlinear temperature effects indicate severe damages to US crop yields under climate change." *Proceedings of the National Academy of sciences* 106(37):15594–15598.

Spenkuch, Jörg L and David Toniatti. 2018. "Political advertising and election results." *The Quarterly Journal of Economics* 133(4):1981–2036.

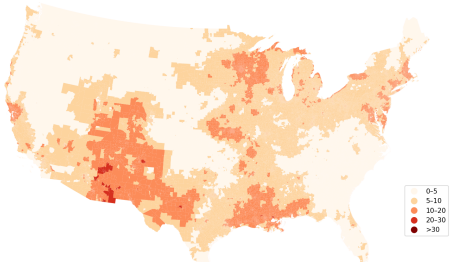
Stokes, Leah C. 2016. "Electoral backlash against climate policy: A natural experiment on retrospective voting and local resistance to public policy." *American Journal of Political Science* 60(4):958–974.

Urpelainen, Johannes and Alice Tianbo Zhang. 2022. "Electoral backlash or positive reinforcement? Wind power and congressional elections in the United States." *The Journal of Politics* 84(3):1306–1321.

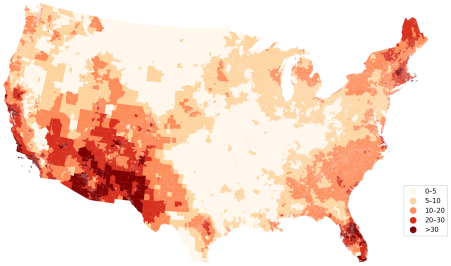
Voorheis, John, Nolan McCarty and Boris Shor. 2015. "Unequal incomes, ideology and gridlock: How rising inequality increases political polarization." *Ideology and Gridlock: How Rising Inequality Increases Political Polarization (August 21, 2015)* .

Wiliam, Dylan and Marnie Thompson. 2017. Integrating assessment with learning: What will it take to make it work? In *The future of assessment*. Routledge pp. 53–82.

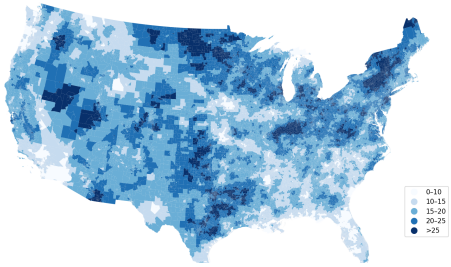
Figure 1: Maps showing main independent variables in 2000 and 2020



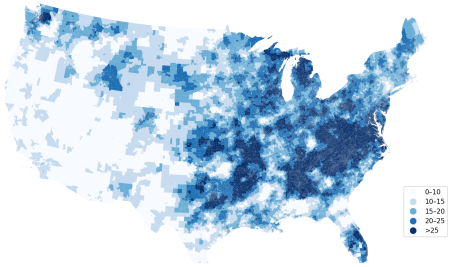
(a) Extreme temperature measure 2000



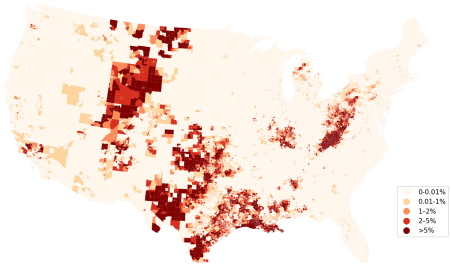
(b) Extreme temperature measure 2020



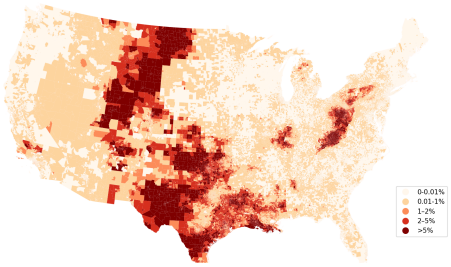
(c) Extreme Precipitation 2000



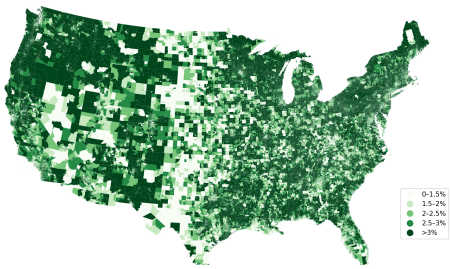
(d) Extreme Precipitation 2020



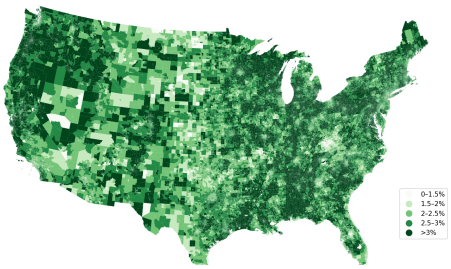
(e) Brown jobs 2000



(f) Brown jobs 2020



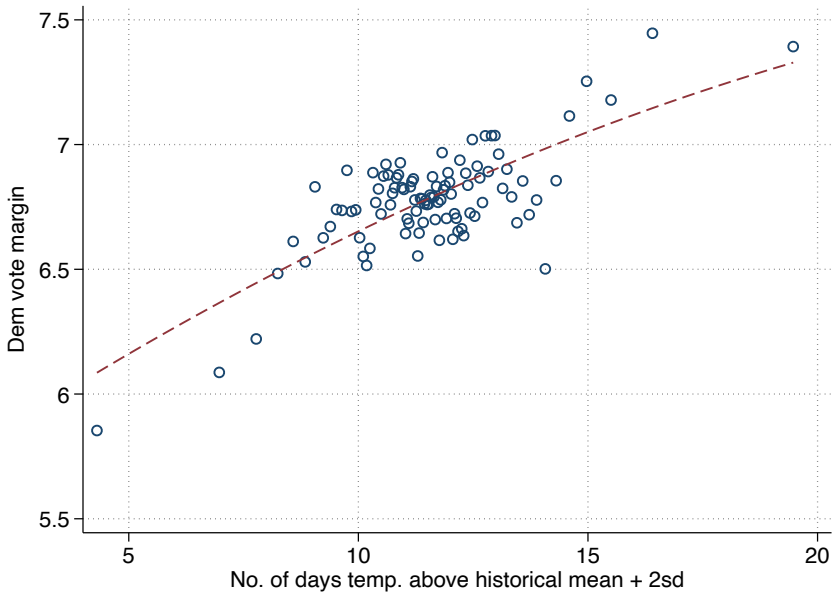
(g) Green jobs 2000



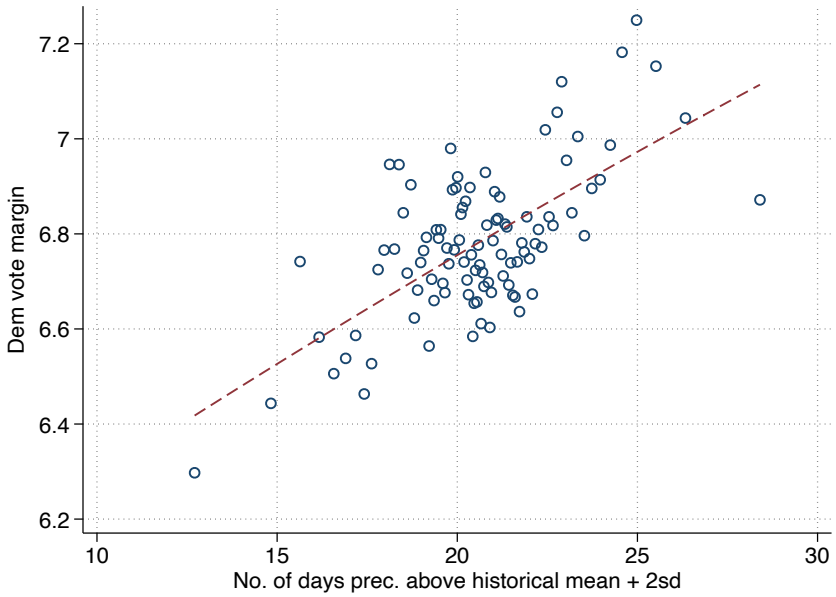
(h) Green jobs 2020

Notes: Each panel shows the spatial distribution of our main exogenous variables of interest in 2000 (left) and 2020 (right), as defined in Section 2. The extreme temperature and precipitation measures are defined

Figure 2: The Relationship Between Extreme Temperature and Precipitation and Democratic Vote Margin



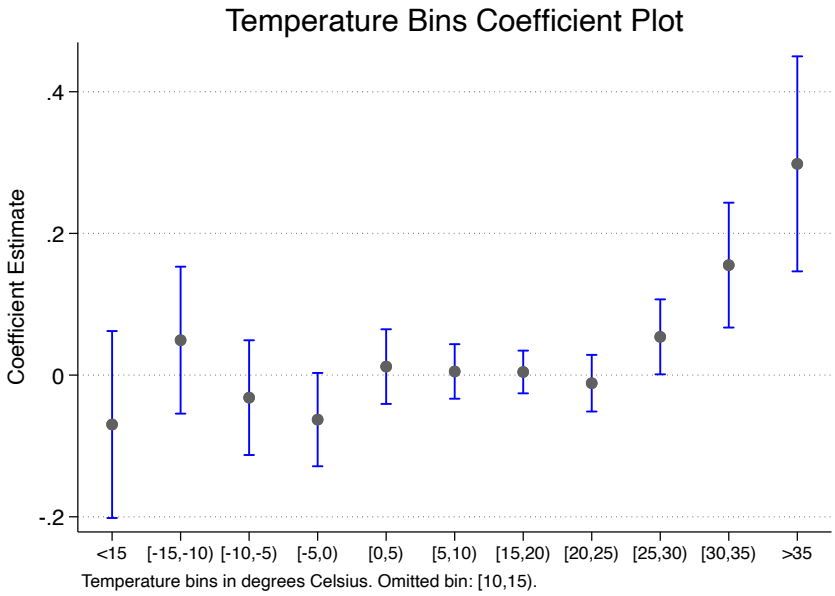
(a) Extreme Temperature (2+SD Above Historical Average)



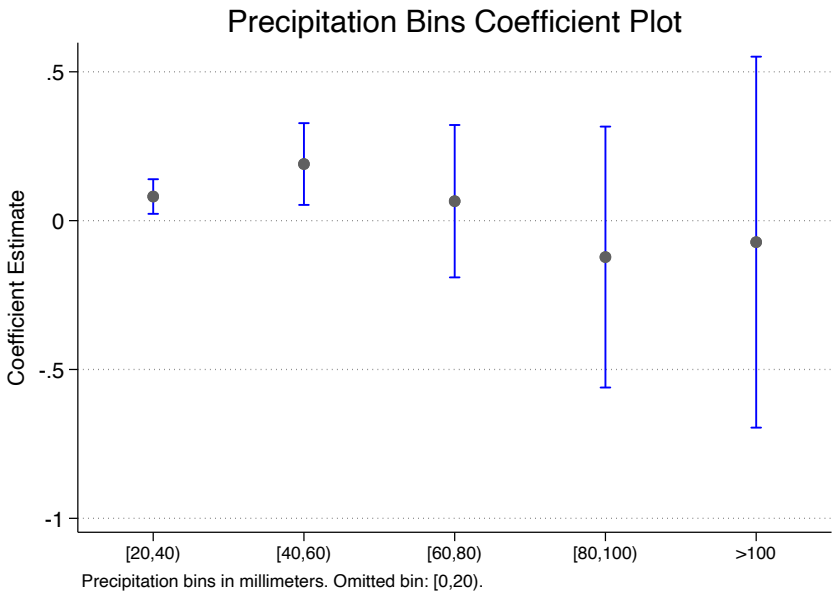
(b) Extreme Precipitation (2+SD Above Historical Average)

Notes: Each panel is a binned scatter plot showing block group-year-level Democratic vote margin as a function of extreme temperature or precipitation, controlling for block-group and Congressional-district-by-year fixed effects. Each dot represents 1% of the sample. The x-axis is extreme temperature or precipitation, defined as number of days in the year above the historical mean plus two standard deviations. The y-axis is the Democratic vote margin in the Congressional election. The red dotted lines are quadratic fits. The sample is Congressional elections from 2000 to 2020. Appendix Figure A.9 shows the same relationships using average temperature and average precipitation. Appendix Figure A.10 shows the same specification using only block-group and year FE.

Figure 3: The Relationship Between Temperature and Precipitation Bins and Democratic Vote Margin



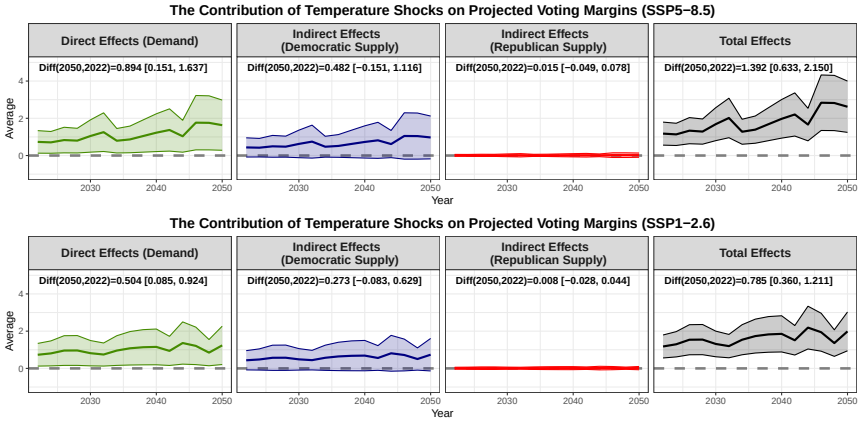
(a) Temperature



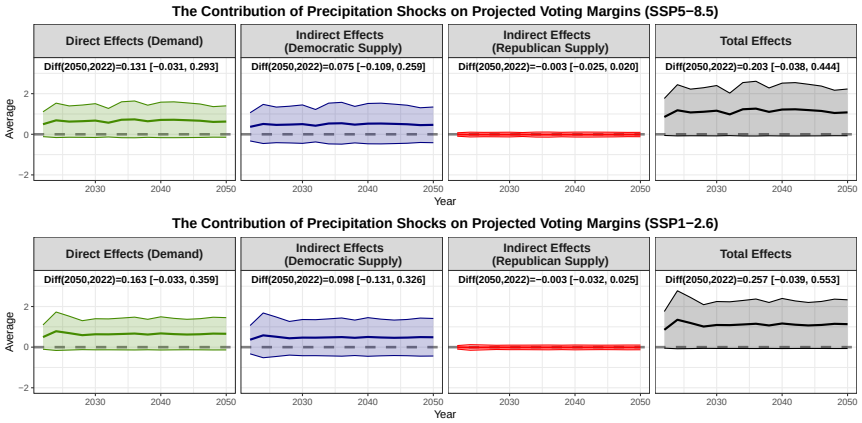
(b) Precipitation

Notes: Each panel shows estimates of the coefficients on bins of temperature or precipitation from a single regression at the precinct-year level where the dependent variable is Democratic vote margin. Each dot represents 1% of the sample. The regression also includes block-group and Congressional-district-by-year fixed effects, the shares of green and brown jobs, and a set of controls. The sample is Congressional elections from 2000 to 2020. The graphs plot coefficients with 95% confidence intervals calculated using standard errors clustered two ways, by block group and Congressional-district-by-year.

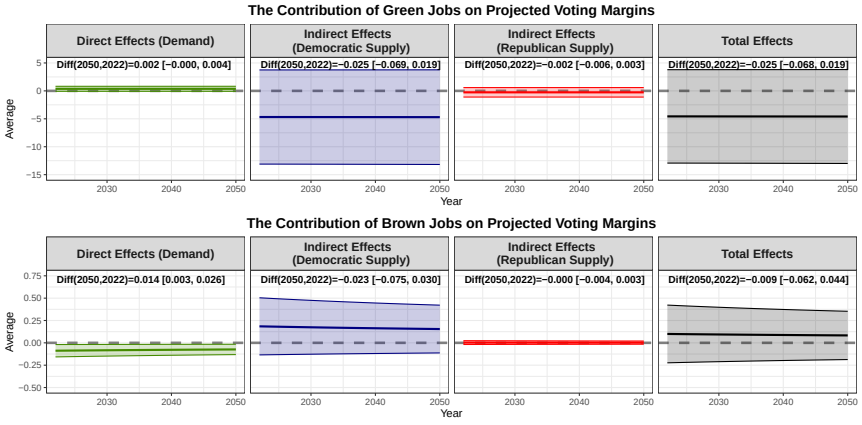
Figure 4: Contribution of weather shocks and employment shifts to projected Democratic vote margins



(a) Temperature Shock



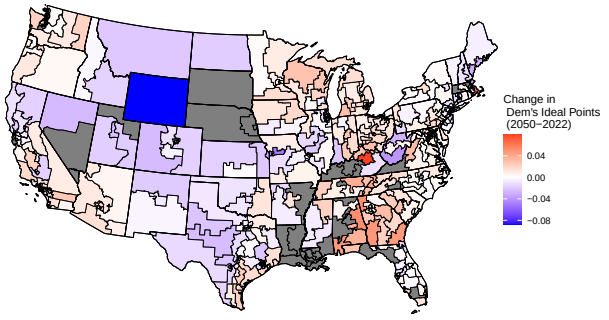
(b) Precipitation Shock



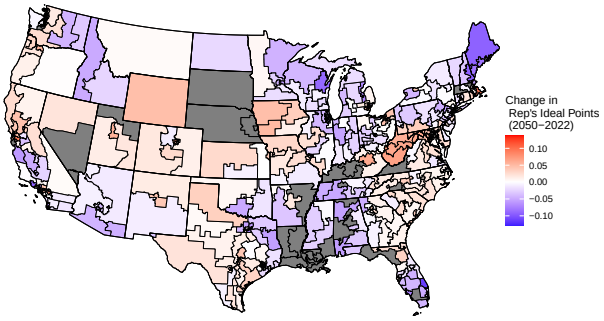
(c) Employment Shifts

Notes: Each panel shows the projected contribution of each exogenous shock on the Democratic vote margins from 2022 to 2050, studying separately the direct and indirect effects of each shock. The indirect effects are those operating through endogenous candidate responses, which themselves affect vote shares. Total effects appear in column 4. Above each plot we report the 2022–2050 difference with 95% confidence intervals, obtained via a 5,000-round bootstrap. For temperature and precipitation, we plot both SSP5-8.5 ("business as usual") and SSP1-2.6 ("optimistic") scenarios from NEX-GDDP. Job projections come from the BLS Occupational Outlook, as described in Section 2. Appendix Figure A.17 shows the evolution of each exogenous variable over the same period.

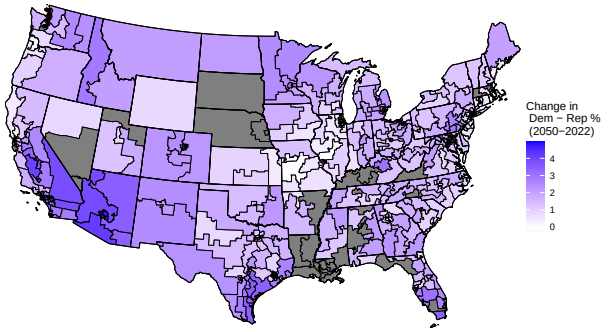
Figure 5: Projected congressional-district shifts from 2022 to 2050.



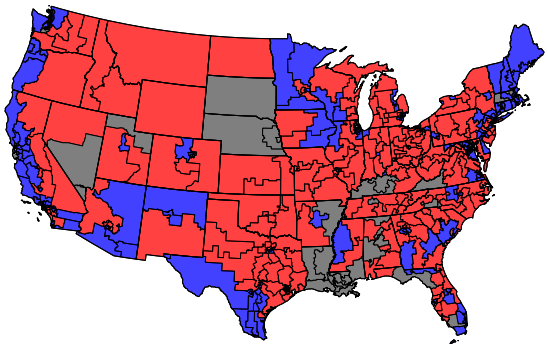
(a) Change in Democrats' ideal ideological position, 2022–2050.



(b) Change in Republicans' ideal ideological position, 2022–2050.



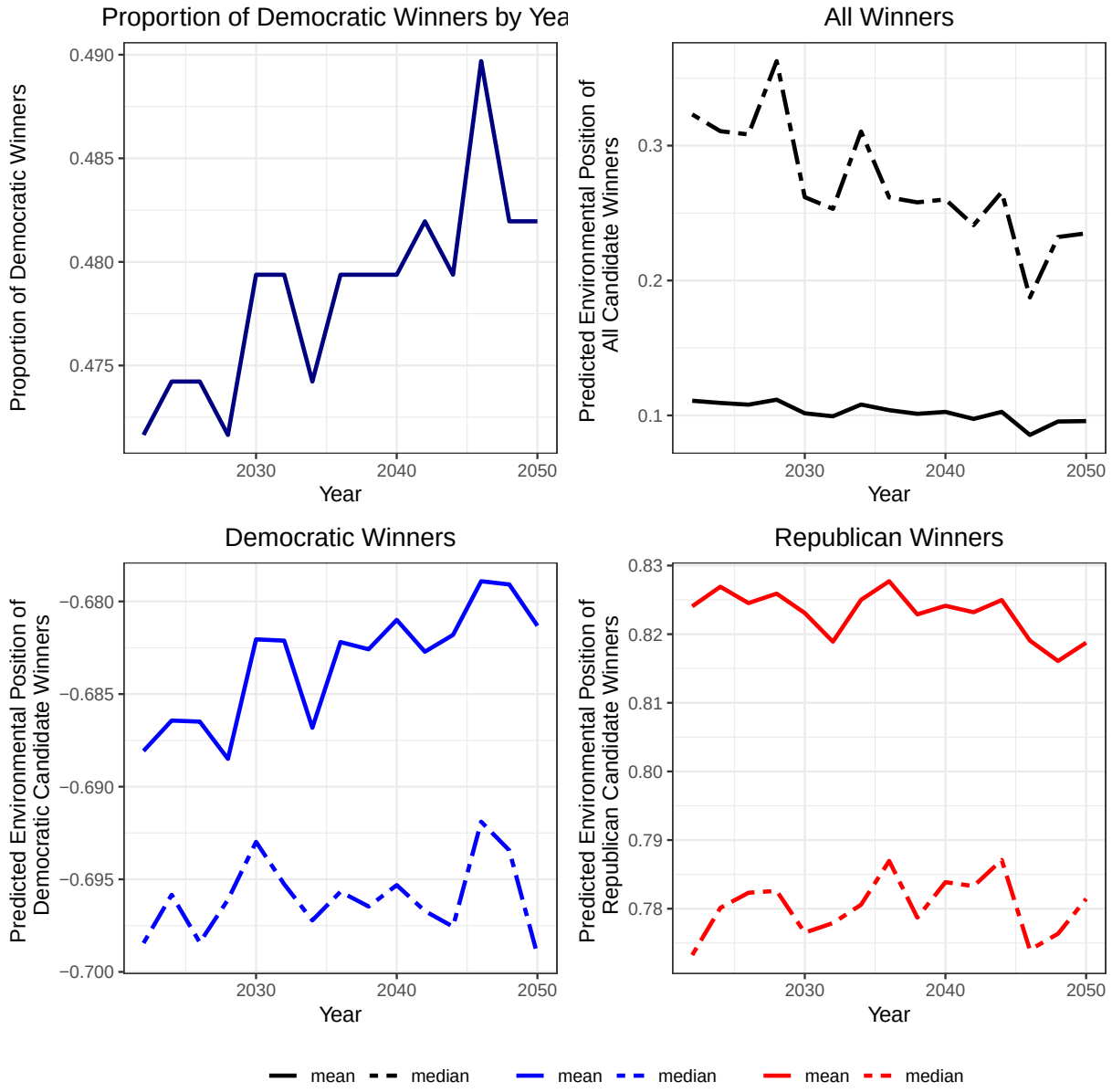
(c) Change in Democratic vote-share margin, 2022–2050.



(d) Projected winning party by district in 2050.

Notes: Each panel shows the projected congressional-district shifts from 2022 to 2050 for the main outcomes of interest, synthesizing the effect of each exogenous shock. Panel A and B show the projected changes in candidate positions. Panel C shows the projected change in the Democratic vote margin. Panel D shows the projected election winner in each congressional district in 2050. Appendix Figure A.19 shows the effect of each shock on the vote margin, including confidence intervals on the state level. Appendix Figure A.20 shows the same results using a hexagonal cartogram.

Figure 6: Projected Composition of the House of Representative



Notes: Each panel shows a projected change in the House of Representatives composition between 2022 and 2050, under the SSP5-8.5 scenario. Panel A plots the proportion of seats won by the Democratic Party in each election cycle. Panel B shows the average and median ideology of all House members. Panels C and D break out the average and median ideology of the Democratic and Republican caucuses, respectively.

Table 1: Within-District Estimates of Voter Demand on Climate Shocks

Dep. var.: Dem-Rep vote share	TWFE	Three-Way FE	FE		TWFE: Conley SE		
	(1)	(2)	(3)	(4)	(5)	(6)	(7)
No. of days temp. above historical mean + 2sd	0.0814***	0.0717***	0.451***	0.412***	0.0853***	0.0853***	0.0853***
	(0.0224)	(0.0236)	(0.0470)	(0.0479)	(0.0215)	(0.0246)	(0.0284)
No. of days prec. above historical mean + 2sd	0.0420**	0.0488**	0.139***	0.187***	0.0428**	0.0428**	0.0428**
	(0.0209)	(0.0208)	(0.0419)	(0.0417)	(0.0186)	(0.0191)	(0.0194)
District x Year FE	X	X	X	X	X	X	X
Block group FE	X	X			X	X	X
DMA x Year FE		X					
Polynomial in Lat. and Lon.				X			
Controls	X	X	X	X	X	X	X
Conley SE Cutoff					25km	50km	100km
Total Effect of 1SD Climate Shocks	0.943***	0.911***	4.592***	4.592***	0.978***	0.978***	0.978***
	(0.220)	(0.233)	(0.457)	(0.462)	(0.214)	(0.237)	(0.264)
Observations	1,339,268	1,333,270	1,348,063	1,333,236	1,333,224	1,333,224	1,333,224

Notes: Each column shows the effects of climate shocks on voter demand from separate regressions. The unit of observation is a block-group-year, and the sample period is 2000 to 2020. The dependent variable is the vote share of the Democratic candidate minus that of the Republican candidate in percentage points. The regression in column (2) includes, in addition to district-year and block-group fixed effects, fixed effects at designated-market-area-year level. The polynomial in latitude and longitude is of degree six. The regressions in columns (5) to (7) have standard errors that account for spatial correlation (Conley (1999)). Rows displaying total effects of a one standard deviation climate shocks are sums of the absolute values of effects of a one standard deviation increase in the two climate shocks. Standard errors are clustered by block-group and district-year, except for in column (2), where they are clustered by block-group, district-year, and DMA-year; they are shown in parentheses. * $p < .10$, ** $p < .05$, *** $p < .01$.

Table 2: Within-District Estimates of Voter Demand on Climate and Jobs Shocks

Dep. var.: Dem-Rep vote share	TWFE	Three-Way FE	TWFE: Conley SE	FE		TWFE +IV	FE + IV
	(1)	(2)	(3)	(4)	(5)	(6)	(7)
No. of days temp. above historical mean + 2sd	0.0822***	0.0717***	0.0861***	0.445***	0.411***	0.0778***	0.432***
	(0.0224)	(0.0236)	(0.0285)	(0.0468)	(0.0476)	(0.0226)	(0.0479)
No. of days prec. above historical mean + 2sd	0.0421**	0.0489**	0.0429**	0.118***	0.167***	0.0466**	0.136***
	(0.0209)	(0.0208)	(0.0195)	(0.0419)	(0.0418)	(0.0214)	(0.0439)
Share Brown Jobs	-0.356***	-0.276***	-0.355***	-0.862***	-1.058***	-0.753	-1.759*
	(0.0839)	(0.0843)	(0.118)	(0.0976)	(0.0988)	(0.600)	(1.051)
Share Green Jobs	0.339***	0.371***	0.368**	-3.953***	-3.990***	6.395***	5.329***
	(0.112)	(0.118)	(0.157)	(0.242)	(0.241)	(2.154)	(1.999)
District x Year FE	X	X	X	X	X	X	X
Block group FE	X	X	X			X	
DMA x Year FE		X					
Polynomial in Lat. and Lon.					X		
Controls	X	X	X	X	X	X	X
Conley SE Cutoff			100km				
F-stat						47.279	11.746
Total Effect of 1SD Climate Shocks	0.951***	0.912***	0.985***	4.402***	4.452***	0.957***	4.476***
	(0.220)	(0.232)	(0.265)	(0.454)	(0.460)	(0.227)	(0.471)
Total Effect of 1SD Jobs Shocks	0.834***	0.715***	0.852***	3.964***	4.341***	5.333***	6.466**
	(0.158)	(0.156)	(0.229)	(0.236)	(0.236)	(1.842)	(2.685)
Observations	1,339,268	1,333,270	1,333,224	1,348,063	1,333,236	1,270,712	1,272,426

Notes: Each column shows the effects of climate and job shocks on voter demand from separate regressions. The unit of observation is a block-group-year, and the sample period is 2000 to 2020. The dependent variable is the vote share of the Democratic candidate minus that of the Republican candidate in percentage points. Share brown jobs and share green jobs are in percentage points. The regression in column (2) includes, in addition to district-year and block-group fixed effects, fixed effects at designated-market-area-year level. The regression in column (3) has standard errors that account for spatial correlation (Conley (1999)). The polynomial in latitude and longitude is of degree six. The regressions in columns (6) and (7) instrument for share brown jobs and share green jobs with their respective shift-share instruments as described in section 3.2. Rows displaying total effects of a one standard deviation climate or jobs shocks are sums of the absolute values of effects of a one standard deviation increase in the two climate shocks or the two jobs shocks. Standard errors are clustered by block-group and district-year, except for in column (2), where they are clustered by block-group, district-year, and DMA-year; they are shown in parentheses. * $p < .10$, ** $p < .05$, *** $p < .01$.

Table 3: Structural Parameter Estimates

Name	Estimate	Std Error	Z-value	P-value	Effects
			Democrat's Supply		
λ^d_{temp}	0.0020*	0.0011	1.7336	0.0830	0.0157
λ^d_{prec}	0.0013	0.0014	0.9517	0.3412	0.0085
λ^d_G	-0.1100	0.1083	-1.0155	0.3099	-0.0426
λ^d_B	0.0301	0.0292	1.0298	0.3031	0.0339
β^d	-0.0195	0.0123	-1.5884	0.1122	-0.6257
π^d	0.1837**	0.0795	2.3091	0.0209	0.0424
			Republican's Supply		
λ^r_{temp}	-0.0008	0.0015	-0.5163	0.6057	-0.0060
λ^r_{prec}	0.0007	0.0021	0.3208	0.7483	0.0042
λ^r_G	0.1144	0.0999	1.1451	0.2522	0.0443
λ^r_B	-0.0089	0.0241	-0.3696	0.7117	-0.0100
β^r	0.0035**	0.0014	2.5740	0.0101	0.1121
π^r	0.1972***	0.0602	3.2773	0.0010	0.0548
			District-level Demand		
δ_{temp}	0.0828***	0.0245	3.3789	0.0007	0.6538
δ_{prec}	0.0443*	0.0231	1.9190	0.0551	0.2833
δ_G	0.2160*	0.1174	1.8389	0.0660	0.0837
δ_B	-0.3562***	0.0927	-3.8428	0.0001	-0.4016
γ^d	24.8117*	12.9817	1.9113	0.0560	8.6327
γ^r	-1.3158	1.0550	-1.2472	0.2123	-0.5654

Notes: This table presents parameter estimates from the structural equations of Democrats' policy supply $\left(x^d_{ct}\right)$, Republicans' policy supply $\left(x^r_{ct}\right)$, and district-level Democratic vote share $\left(\bar{y}_{ct}\right)$. Standard errors (in parentheses) are clustered by congressional district; z-values and p-values reflect two-sided tests. The final column ("Marginal Effects") indicates the change in the outcome—Democrats' platform in the first panel, Republicans' platform in the second panel, and Democrats' vote share (on a 0–100 scale) in the third panel—arising from a one-standard-deviation increase in the corresponding regressor. Estimation uses a two-step GMM approach with instruments $\bar{\mathbf{V}}_{ct}, z^d_{ct}, z^r_{ct}$, and weighting by the inverse variance of the estimated district-by-year fixed effects in the first step. A single asterisk $(*)$ indicates significance at the 10% level; two asterisks $(**)$ at the 5% level; and three asterisks $(***)$ at the 1% level.

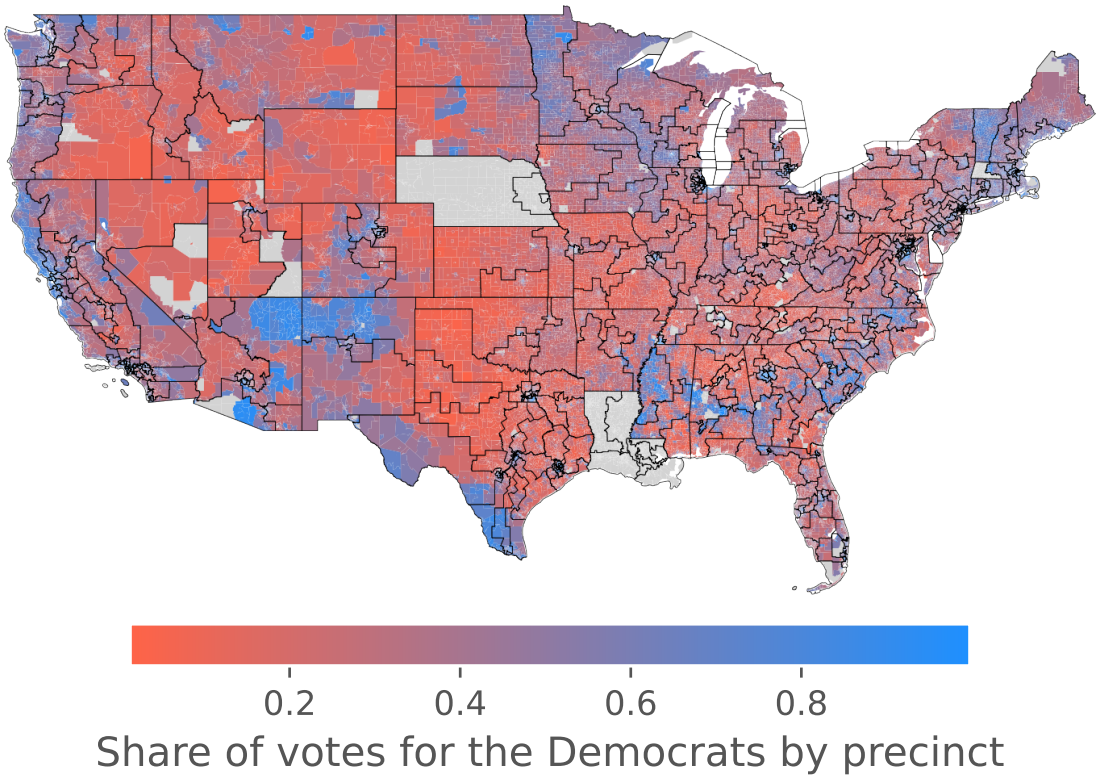
Table 4: Reduced-form District-Year Level Estimates

	Democrat's Vote Share			**Democrat's Position**			**Republican's Position**		
	Direct (1)	Indirect (2)	Total (3)	Direct (4)	Indirect (5)	Total (6)	Direct (7)	Indirect (8)	Total (9)
Temperature	0.056**	0.034*	0.089***	-0.002*	0.002*	0.000	0.000**	-0.001	-0.000
	(0.024)	(0.020)	(0.024)	(0.001)	(0.001)	(0.001)	(0.000)	(0.001)	(0.001)
Precipitation	0.030	0.021	0.051*	-0.001	0.001	0.000	0.000	0.001	0.001
	(0.018)	(0.022)	(0.028)	(0.001)	(0.001)	(0.001)	(0.000)	(0.002)	(0.002)
Brown Jobs	-0.239**	0.509	0.270	-0.005	0.030	0.025	0.001	-0.009	-0.008
	(0.095)	(0.446)	(0.452)	(0.011)	(0.030)	(0.023)	(0.002)	(0.024)	(0.024)
Green Jobs	0.145	-1.933	-1.788	0.035	-0.110	-0.075	-0.006	0.114	0.108
	(0.092)	(1.625)	(1.657)	(0.059)	(0.107)	(0.063)	(0.005)	(0.101)	(0.101)

Notes: This table reports the direct, indirect, and total reduced-form coefficients of temperature, precipitation, brown jobs, and green jobs on three outcomes: Democratic vote share, the Democrat's policy position, and the Republican's policy position. When the outcome is the Democratic vote share $(\bar{y}_{ct})$, the "direct effect" corresponds to the $\Xi\,\delta$ term, and the "indirect effect" corresponds to $\Xi(\gamma^d\lambda^d + \gamma^r\lambda^r)$. For the Democrat's policy position (x^d_{ct}), the direct effect is λ^d, while the indirect effect is $\beta^d\Xi(\delta + \gamma^d\lambda^d + \gamma^r\lambda^r)$. An analogous decomposition applies to the Republican's policy position (x^r_{ct}). Standard errors (in parentheses) are constructed using the structural parameter estimates and are clustered at the congressional-district level. A single asterisk $(*)$ indicates significance at the 10% level; two asterisks $(**)$ at the 5% level; and three asterisks $(***)$ at the 1% level.

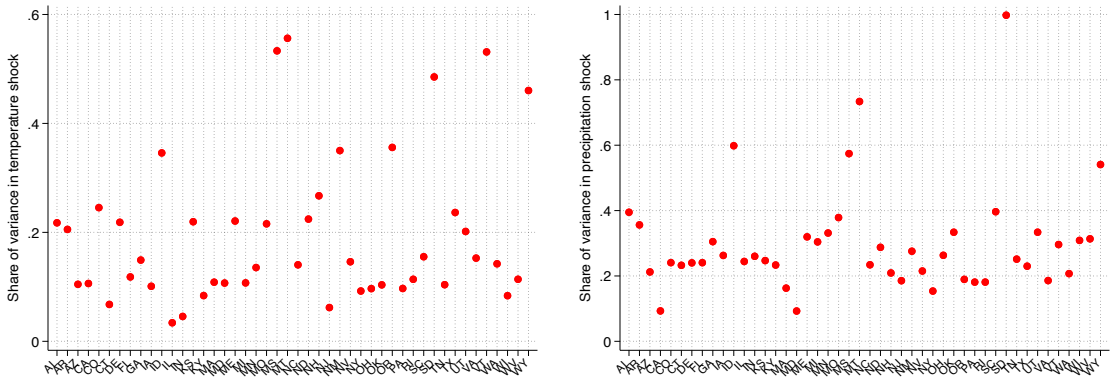
A Online Appendix for "Climate Politics in the United States", by M. Bombardini, F. Finan, N. Longuet-Marx, S. Naidu, F. Trebbi

Figure A.7: Map of precinct-level voting patterns in 2020 (from Longuet-Marx (2024)).



Notes: The figure shows the Democratic vote share in the 2020 House election for each census block group, overlaid with congressional district boundaries. Data are as described in Section 2.

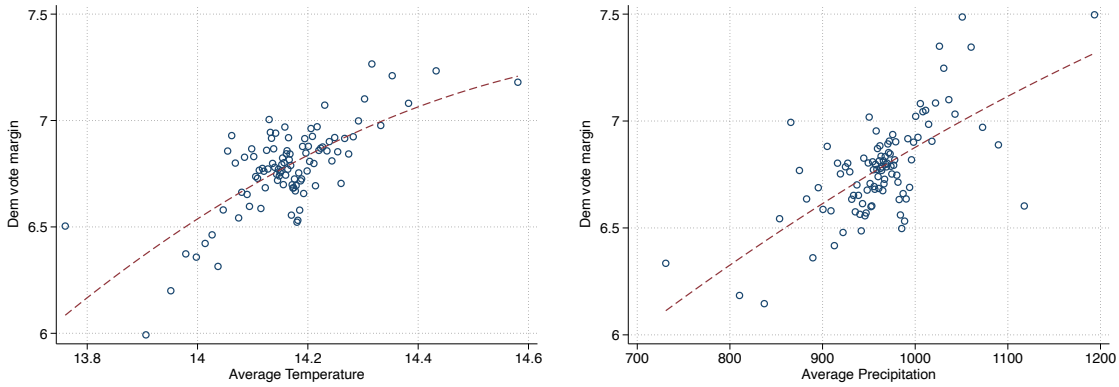
Figure A.8: Residual Variation in Temperature and Precipitation Shocks after partialling out for Congressional District x Year fixed effects



(a) Temperature Shock (b) Precipitation Shock

Notes: Each point represents, for each state, the share of the variance of the temperature and precipitation shock variable after partialling out Congressional District × Year fixed effects.

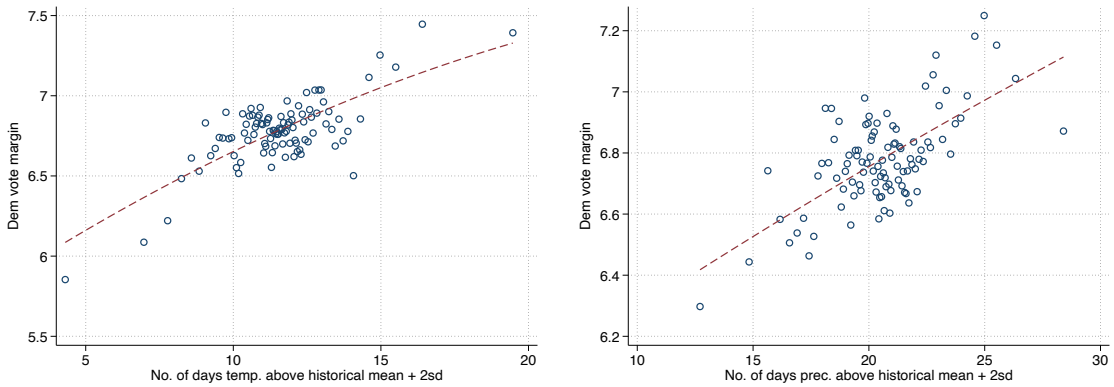
Figure A.9: The Relationship Between Average Temperature and Precipitation and Democratic Vote Margin



(a) Average Temperature (b) Average Precipitation

Notes: Each panel is a binned scatter plot showing block-group-year-level Democratic vote margin as a function of average temperature or precipitation, controlling for block-group and Congressional-district-by-year fixed effects. Each dot represents 1% of the sample. The x-axis is average temperature or precipitation. The y-axis is the Democratic vote margin in the Congressional election. The red dotted lines are quadratic fits. The sample is Congressional elections from 2000 to 2020.

Figure A.10: The Relationship Between Extreme Temperature and Precipitation and Democratic Vote Margin, controlling only for block-group and year fixed effects

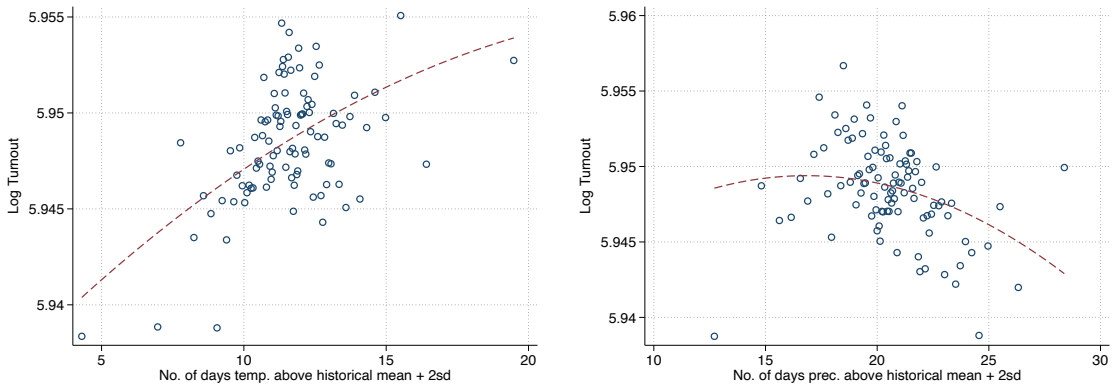


(a) Extreme Temperature (2+SD Above Historical Average)

(b) Extreme Precipitation (2+SD Above Historical Average)

Notes: As in Figure 2, each panel is a binned scatterplot showing block group-year-level Democratic vote margin as a function of extreme temperature or precipitation, controlling for block-group and Congressional-district-by-year fixed effects. Each dot represents 1% of the sample. The x-axis is extreme temperature or precipitation, defined as number of days in the year above the historical mean plus two standard deviations. The y-axis is the Democratic vote margin in the Congressional election. The red dotted lines are quadratic fits. The sample is Congressional elections from 2000 to 2020.

Figure A.11: The Relationship Between Extreme Temperature and Precipitation and Voter Turnout

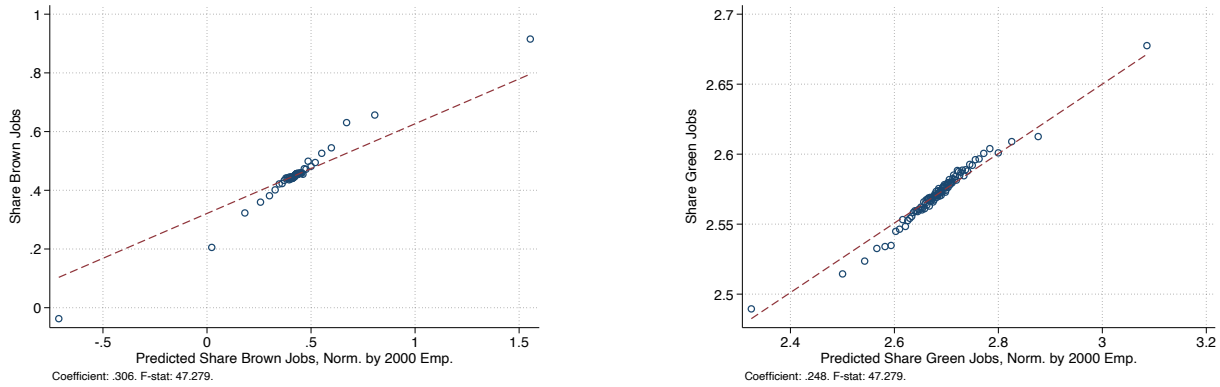


(a) Extreme Temperature (2+SD Above Historical Average)

(b) Extreme Precipitation (2+SD Above Historical Average)

Notes: Each panel is a binned scatter plot showing precinct-year-level voter turnout as a function of extreme temperature or precipitation, controlling for block-group and Congressional-district-by-year fixed effects. Each dot represents 1% of the sample. The x-axis is extreme temperature or precipitation, defined as number of days in the year above the historical mean plus two standard deviations. The y-axis is the log of voter turnout in the Congressional election. The red dotted lines are quadratic fits. The sample is Congressional elections from 2000 to 2020.

Figure A.12: First Stage Relationships for Green and Brown Jobs

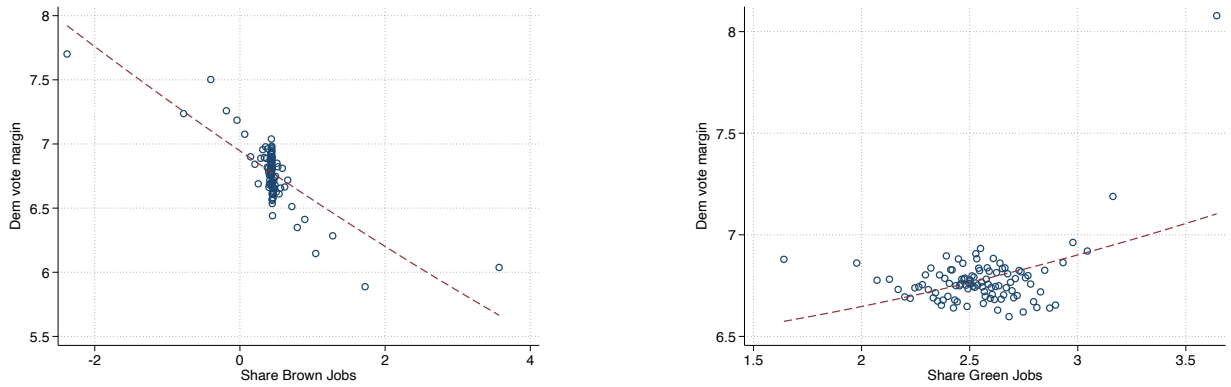


(a) First Stage for Brown Jobs

(b) First Stage for Green Jobs

Notes: Each panel is a binned scatter plot showing the first-stage relationship between the shift-share instruments and brown or green jobs at the precinct-year level. Each dot represents 1% of the sample. Each binned scatter plot controls for block-group and Congressional-district-by-year fixed effects, extreme temperature and precipitation as measured by number of days in the year above the historical mean plus two standard deviations, and a set of controls. The x-axis is the shift-share instrument, which is the predicted share of jobs in oil, gas, and coal–or the predicted share of green jobs–normalized by total employment in 2000. The y-axis is the share of jobs in oil, gas, and coal; or the share of green jobs. The red dotted lines are linear fits. The sample is Congressional elections from 2000 to 2020.

Figure A.13: The Relationship Between Brown and Green Jobs and Democratic Vote Margin

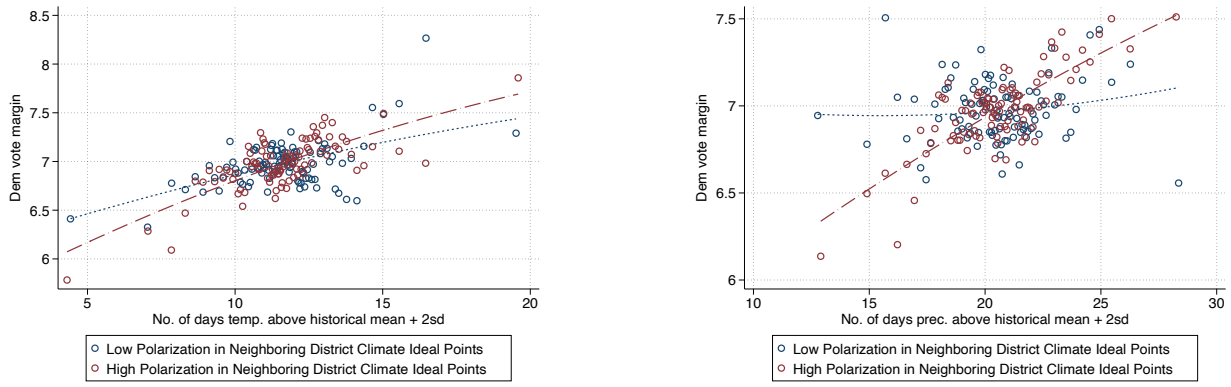


(a) Brown Jobs

(b) Green Jobs

Notes: Each panel is a binned scatter plot showing block group-year-level Democratic vote margin as a function of brown or green jobs. Each binned scatter plot controls for block-group and Congressional-district-by-year fixed effects. Each dot represents 1% of the sample. The x-axis is share of jobs in oil, gas, and coal; or share of green jobs. The y-axis is the Democratic vote margin in the Congressional election. The red dotted lines are quadratic fits. The sample is Congressional elections from 2000 to 2020.

Figure A.14: Heterogeneity of Climate Variable Effect by Partisan Difference in Supply-Shifter.



(a) Temperature

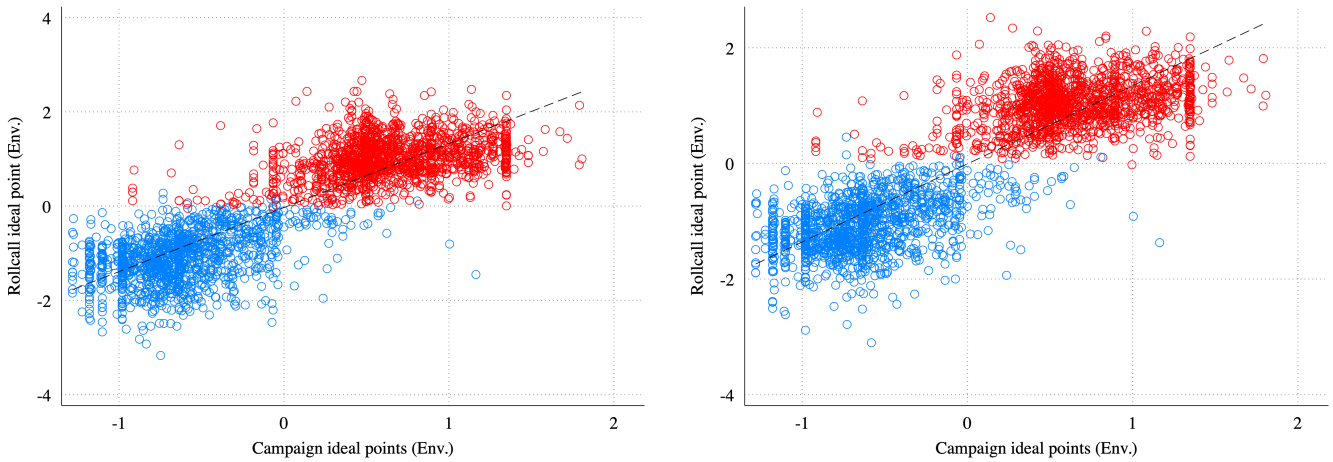
(b) Precipitation

Notes: Each panel is a binned scatter plot showing precinct-year-level Democratic vote margin as a function of brown or green jobs. Each dot represents 1% of the sample. Each binned scatter plot controls for block-group and Congressional-district-by-year fixed effects and the residuals from a first-stage regression of brown or green jobs on its shift-share instrument. The x-axis is share of jobs in oil, gas, and coal; or share of green jobs. The y-axis is the Democratic vote margin in the Congressional election. The red dotted lines are quadratic fits. The sample is Congressional elections from 2000 to 2020.

Figure A.15: The Relationship Between Environmental Campaign Ideal Points and Vote-based Ideology Measures

(a) Narrow Environment Definition

(b) Broad Environment Definition

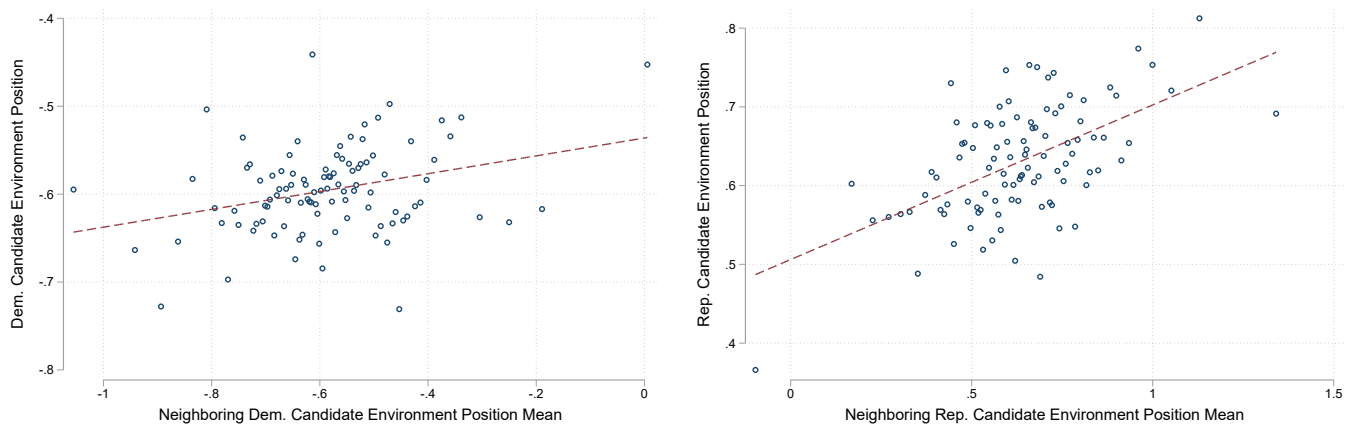


Notes: The "narrow" definition uses Comparative Agendas Project (CAP) codes 700 (environment) and 800 (energy). The "broad" definition adds 400 (agriculture), 1000 (transportation), disaster relief (1523), and hazardous waste in military (1614) along with technology categories (1704,1706, and 1708 (commercial use of space, telecommunications, and weather forecasting), foreign resource exploitation (1902) as well as most of 2100 (Public lands, omitting indigenous affairs and dependencies and territories). Ideal points are obtained following Bateman, Katznelson and Lapinski (2018). The sample correlation with the "narrow" definition is 0.866 (0.417 among Democrats and 0.333 among Republicans) and with the "broad" definition is 0.860 (0.421 among Democrats and 0.324 among Republicans).

Figure A.16: Correlation between candidate campaign ideal point on the environment and average ideal point of neighboring candidates of same party.

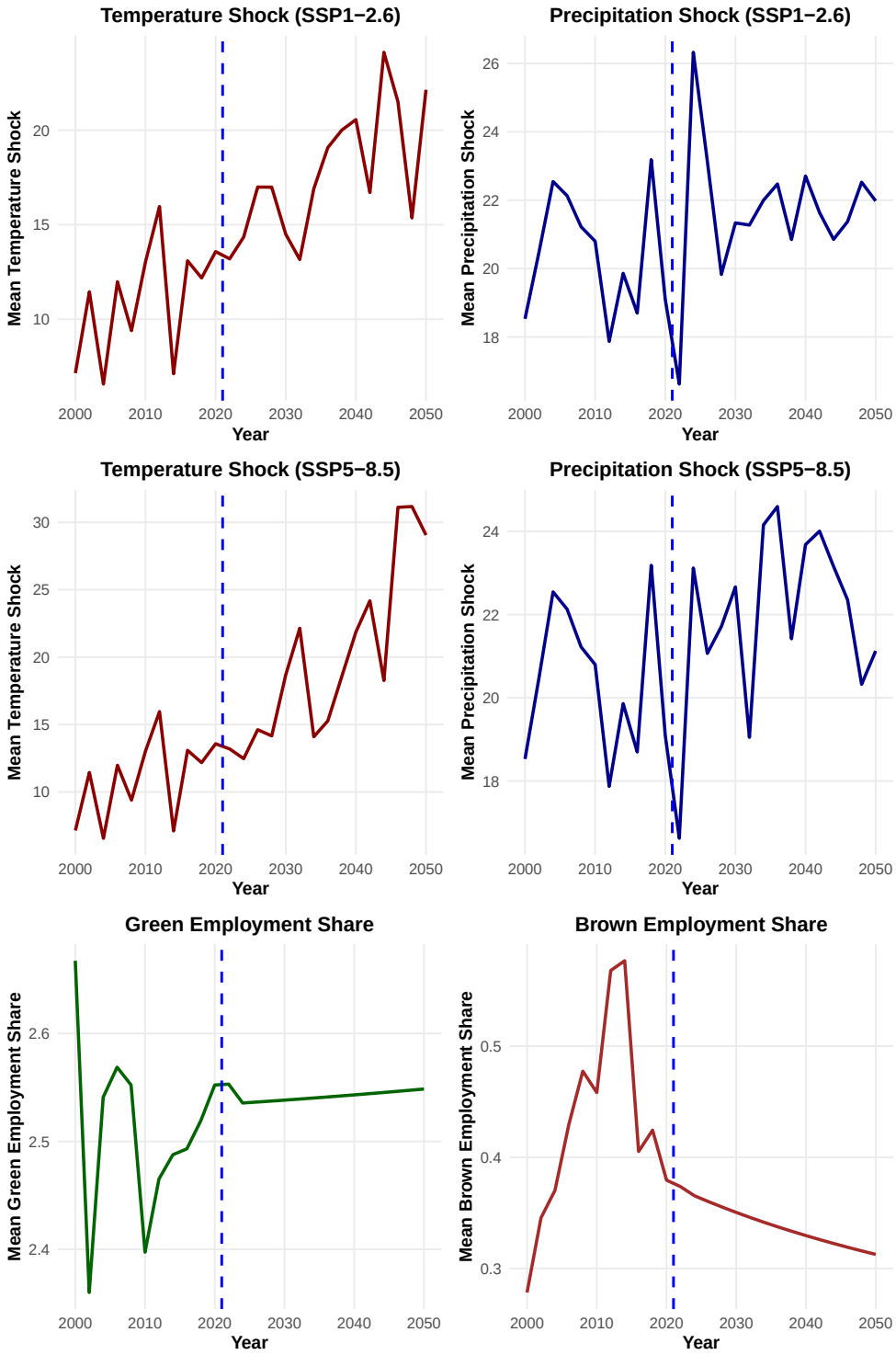
(a) Democratic Representatives

(b) Republican Representatives



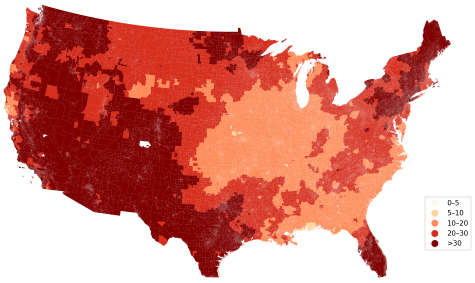
Notes: Each panel is a binned scatter plot showing the first-stage relationship between candidates environmental positions and their neighbors' environmental positioning. Each dot represents 1% of the sample. The red dotted lines are linear fits. The sample is Congressional elections from 2000 to 2020.

Figure A.17: Time series of Sample Averages and Projections of Main Independent Variables.

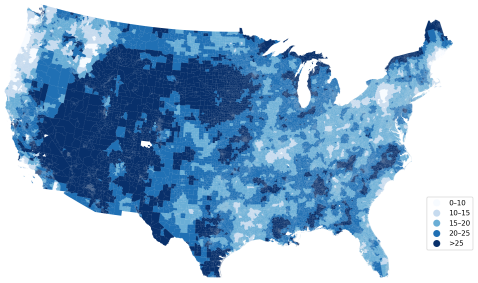


Notes: Sample average and projections of independent variables using SSP1-2.6 and SSP5-8.5 scenarios from 2022 to 20250. The vertical dashed line indicates 2020, the last year of our sample. The projections for jobs come from the BLS Occupational Outlook Handbook.

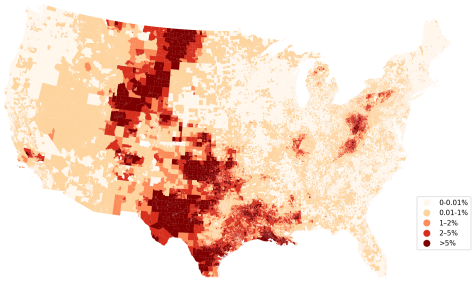
Figure A.18: Maps showing projections of main independent variables in 2050



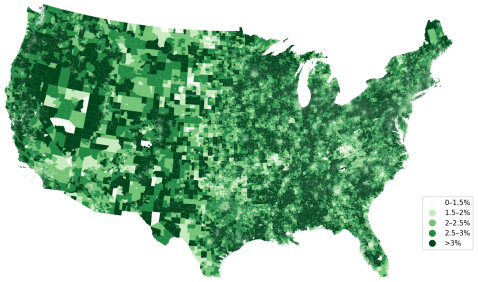
(a) Extreme temperature measure 2050



(b) Extreme Precipitation 2050



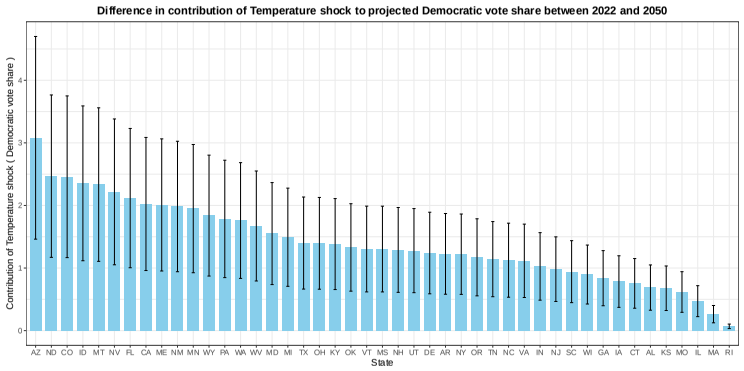
(c) Brown jobs 2050



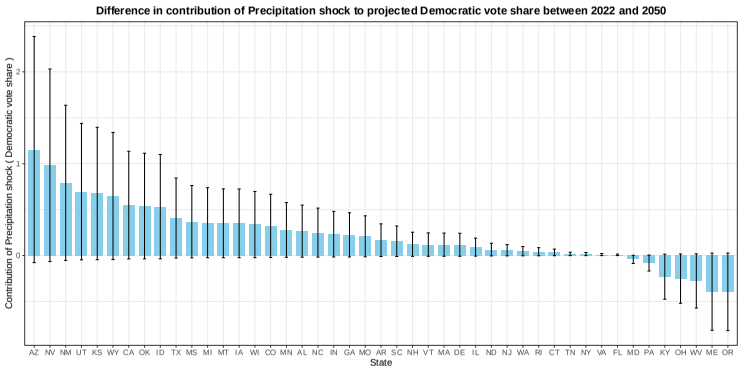
(d) Green jobs 2050

Notes: Each panel shows the spatial distribution of our main exogenous variables of interest in 2050, as defined in Section 2. The extreme temperature and precipitation measures are defined as the number of days in the year above the historical mean plus two standard deviations. The job projections come from the BLS Occupational Outlook Handbook. The temperature and weather projections are projections made under the SSP5-8.5 scenario, which is our preferred scenario.

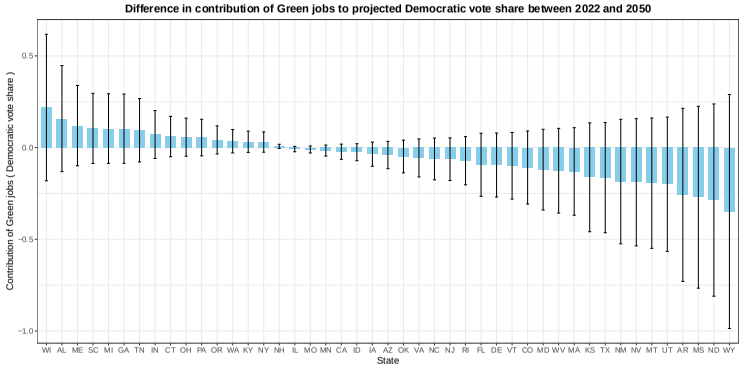
Figure A.19: Projected Democratic Vote Margins By State



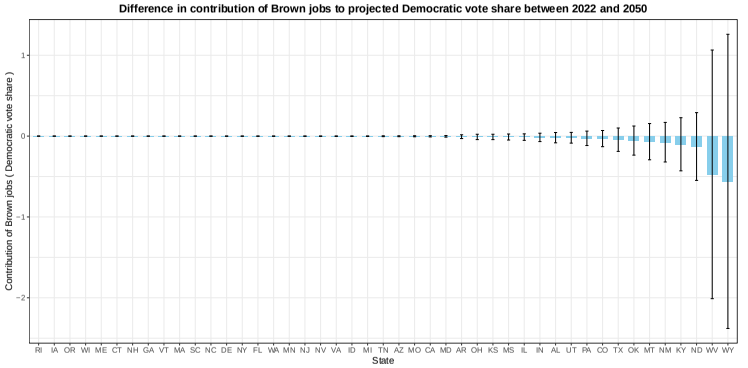
(a) Temperature Shock



(b) Precipitation Shock



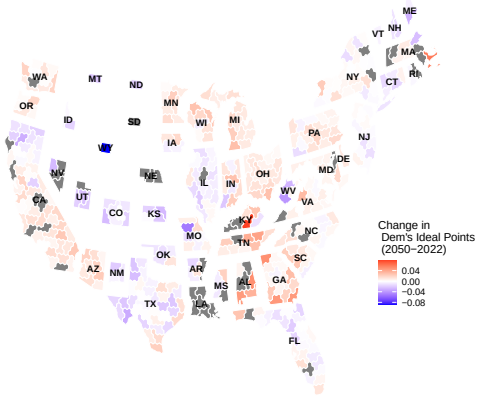
(c) Green Jobs



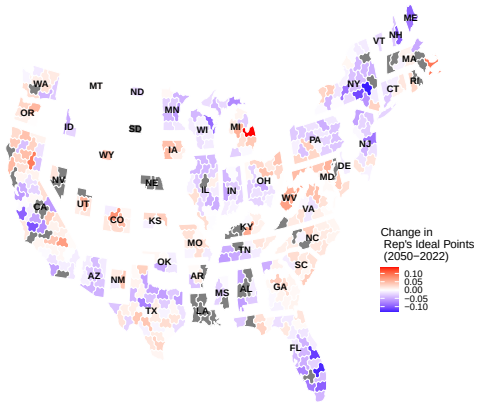
(d) Brown Jobs

Notes: Each panel displays the change in the projected contribution of each exogenous shock to Democratic vote margins between 2022 and 2050, with 95% confidence intervals, separately for every state. The confidence intervals are derived from 5000 bootstrap replications. Temperature and precipitation projections follow the SSP5-8.5 ("business-as-usual") scenario. Job projections come from the BLS Occupational Outlook, as discussed in Section 2.

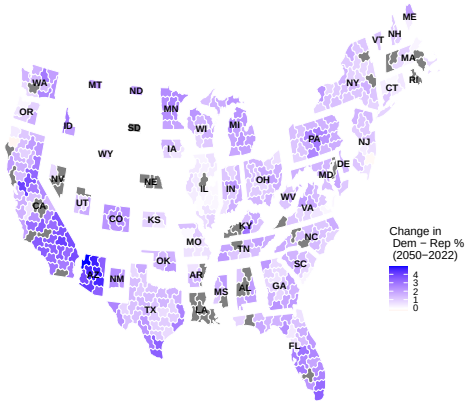
Figure A.20: Hexagonal-cartogram view of projected congressional-district shifts from 2022 to 2050.



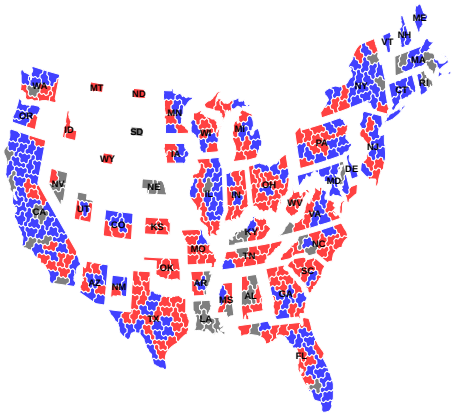
(a) Change in Democrats' ideal ideological position, 2022–2050.



(b) Change in Republicans' ideal ideological position, 2022–2050.



(c) Change in Democratic vote-share margin, 2022–2050.



(d) Projected winning party by district in 2050.

Notes: As in Figure 5, each panel shows the projected congressional-district shifts from 2022 to 2050 for the main outcomes of interest, synthesizing the effect of each exogenous shock. Panel A and B show the projected changes in candidate positions. Panel C shows the projected change in the Democratic vote margin. Panel D shows the projected election winner in each congressional district in 2050.

Table A.5: States and Years Present in Sample

State	Years in Sample
Alabama	2000, 2002, 2004, 2006, 2008, 2010, 2012, 2014, 2016, 2018, 2020
Arizona	2002, 2004, 2006, 2008, 2010, 2012, 2014, 2016, 2018, 2020
Arkansas	2000, 2002, 2004, 2006, 2010, 2012, 2014, 2016, 2018, 2020
California	2000, 2002, 2004, 2006, 2008, 2010, 2012, 2014, 2016, 2018, 2020
Colorado	2004, 2006, 2008, 2010, 2012, 2014, 2016, 2018, 2020
Connecticut	2000, 2002, 2004, 2006, 2008, 2010, 2012, 2014, 2016, 2018, 2020
Delaware	2002, 2004, 2006, 2008, 2010, 2012, 2014, 2016, 2018, 2020
Florida	2006, 2008, 2010, 2012, 2014, 2016, 2018, 2020
Georgia	2012, 2014, 2016, 2018, 2020
Idaho	2000, 2002, 2004, 2006, 2008, 2010, 2012, 2014, 2016, 2018, 2020
Illinois	2012, 2014, 2016, 2018, 2020
Indiana	2012, 2016, 2018, 2020
Iowa	2000, 2004, 2006, 2008, 2010, 2012, 2014, 2016, 2018, 2020
Kansas	2000, 2002, 2004, 2006, 2008, 2010, 2012, 2016, 2018, 2020
Kentucky	2010, 2012, 2014, 2016, 2018, 2020
Maine	2000, 2002, 2004, 2006, 2008, 2010, 2012, 2014, 2016, 2018, 2020
Maryland	2004, 2006, 2008, 2010, 2012, 2014, 2016, 2018, 2020
Massachusetts	2002, 2004, 2006, 2008, 2010, 2012, 2014, 2016, 2018, 2020
Michigan	2000, 2002, 2004, 2006, 2008, 2010, 2012, 2014, 2016, 2018, 2020
Minnesota	2000, 2002, 2004, 2006, 2008, 2010, 2012, 2014, 2016, 2018, 2020
Mississippi	2004, 2006, 2008, 2010, 2012, 2018, 2020
Missouri	2000, 2002, 2004, 2006, 2008, 2010, 2014, 2016, 2018, 2020
Montana	2000, 2002, 2004, 2006, 2008, 2010, 2012, 2014, 2016, 2018, 2020
Nevada	2004, 2006, 2008, 2010, 2018, 2020
New Hampshire	2000, 2002, 2004, 2006, 2008, 2010, 2012, 2014, 2016, 2018, 2020
New Jersey	2000, 2002, 2004, 2008, 2012, 2014, 2016, 2018, 2020
New Mexico	2000, 2004, 2006, 2008, 2010, 2012, 2014, 2016, 2018, 2020
New York	2006, 2008, 2010, 2012, 2014, 2016, 2018, 2020
North Carolina	2000, 2002, 2004, 2006, 2008, 2010, 2012, 2014, 2016, 2018, 2020
North Dakota	2002, 2004, 2006, 2008, 2010, 2012, 2014, 2016, 2018, 2020
Ohio	2004, 2006, 2008, 2010, 2012, 2014, 2016, 2018, 2020
Oklahoma	2002, 2004, 2006, 2008, 2010, 2012, 2014, 2016, 2018, 2020
Oregon	2000, 2002, 2004, 2006, 2008, 2010, 2012, 2014, 2018, 2020
Pennsylvania	2000, 2002, 2004, 2006, 2008, 2010, 2012, 2014, 2016, 2018, 2020
Rhode Island	2000, 2002, 2004, 2006, 2008, 2010, 2012, 2014, 2016, 2018, 2020
South Carolina	2006, 2008, 2010, 2012, 2014, 2016, 2018, 2020
South Dakota	2008, 2016, 2018, 2020
Tennessee	2002, 2004, 2006, 2008, 2010, 2012, 2014, 2016, 2018, 2020
Texas	2000, 2002, 2004, 2006, 2008, 2010, 2012, 2014, 2016, 2018, 2020
Utah	2014, 2016, 2018, 2020
Vermont	2006, 2010, 2012, 2014, 2018, 2020
Virginia	2000, 2002, 2004, 2006, 2008, 2010, 2012, 2014, 2016, 2018, 2020
Washington	2006, 2008, 2010, 2012, 2014, 2016, 2018, 2020
West Virginia	2008, 2010, 2012, 2014, 2016, 2018, 2020
Wisconsin	2002, 2004, 2006, 2008, 2010, 2012, 2014, 2016, 2018, 2020
Wyoming	2000, 2002, 2004, 2006, 2008, 2010, 2012, 2014, 2016, 2018, 2020

Notes: States and years included in the sample.

Table A.6: Robustness of Demand Estimates to Varying Measures of Climate

	(1)	(2)	(3)	(4)
Average Temperature	1.536***		1.604***	
	(0.451)		(0.457)	
No. of days temp. above historical mean + 2sd		0.0821***		0.0839***
		(0.0224)		(0.0227)
No. of days temp. below historical mean - 2sd		0.0598*		0.0587
		(0.0361)		(0.0366)
Average Precipitation	0.00285***		0.00286***	
	(0.000907)		(0.000919)	
No. of days prec. above historical mean + 2sd		0.0381*		0.0391*
		(0.0211)		(0.0213)
District x Year FE	X	X	X	X
Block group FE	X	X	X	X
Controls	Long	Long	None	None
Total Effect of 1SD Climate Shocks	8.060***	1.248***	8.368***	1.263***
	(2.080)	(0.286)	(2.111)	(0.290)
Observations	1,339,268	1,339,268	1,339,268	1,339,268

Notes: Each column shows the effects of climate shocks on voter demand from separate regressions. The unit of observation is a block-group-year, and the sample period is 2000 to 2020. The dependent variable is the vote share of the Democratic candidate minus that of the Republican candidate in percentage points. Total effect of one standard deviation climate shocks is sum of the effects of a one standard deviation increase in all climate shocks. Standard errors are clustered by block-group and district-year and are shown in parentheses. * $p < .10$, ** $p < .05$, *** $p < .01$.

Table A.7: Robustness of Demand Estimates to Varying Measures of Climate

	(1)	(2)	(3)	(4)
Average Temperature	0.989***		3.117***	
	(0.178)		(0.262)	
No. of days temp. above historical mean + 2sd		0.424***		0.682***
		(0.0472)		(0.0616)
No. of days temp. below historical mean - 2sd		-0.501***		-0.952***
		(0.0761)		(0.0993)
Average Precipitation	0.00599***		0.00288**	
	(0.00111)		(0.00132)	
No. of days prec. above historical mean + 2sd		0.181***		0.287***
		(0.0422)		(0.0541)
District x Year FE	X	X	X	X
Block group FE				
Controls	Long	Long	None	None
Total Effect of 1SD Climate Shocks	6.901***	7.369***	15.148***	12.614***
	(0.941)	(0.622)	(1.335)	(0.816)
Observations	1,348,063	1,348,063	1,348,063	1,348,063

Notes: Each column shows the effects of climate shocks on voter demand from separate regressions. The unit of observation is a block-group-year, and the sample period is 2000 to 2020. The dependent variable is the vote share of the Democratic candidate minus that of the Republican candidate in percentage points. Total effect of one standard deviation climate shocks is sum of the effects of a one standard deviation increase in all climate shocks. Standard errors are clustered by block-group and district-year and are shown in parentheses. * $p < .10$, ** $p < .05$, *** $p < .01$.

Table A.8: Heterogeneity of Within-District Demand Estimates by Partisan Difference in Supply-Shifters

	(1)	(2)	(3)	(4)	(5)	(6)
No. of days temp. above historical	0.0704**	0.0688**	0.0702*	0.0673**	0.0658**	0.0618*
mean + 2sd	(0.0274)	(0.0274)	(0.0358)	(0.0264)	(0.0264)	(0.0342)
No. of days prec. above historical	0.0404	0.0355	0.0348	0.0400	0.0357	0.0371
mean + 2sd	(0.0283)	(0.0284)	(0.0344)	(0.0273)	(0.0274)	(0.0330)
Share Brown Jobs		-0.190	-0.400		-0.198	-0.301
		(0.128)	(1.012)		(0.127)	(0.945)
Share Green Jobs		-0.107	37.22***		-0.0201	36.07***
		(0.175)	(7.865)		(0.176)	(7.630)
Republican Minus Democratic Shifter	0.385***	0.337***	0.403***	0.378***	0.331***	0.405***
× No. of days temp. above historical mean + 2sd	(0.0926)	(0.0895)	(0.123)	(0.0938)	(0.0905)	(0.122)
Republican Minus Democratic Shifter	0.178*	0.155*	0.155	0.180*	0.159*	0.159
× No. of days prec. above historical mean + 2sd	(0.0962)	(0.0936)	(0.112)	(0.0933)	(0.0908)	(0.109)
Republican Minus Democratic Shifter		-0.973***	-1.387***		-0.934***	-1.231***
× Share Brown Jobs		(0.284)	(0.463)		(0.284)	(0.452)
Republican Minus Democratic Shifter		-5.529***	9.464***		-5.424***	9.934***
× Share Green Jobs		(0.664)	(3.253)		(0.668)	(3.154)
District x Year FE	X	X	X	X	X	X
Block group FE	X	X	X	X	X	X
Controls	None	None	None	Long	Long	Long
Spec.	TWFE	TWFE	IV	TWFE	TWFE	IV
Observations	1,370,901	1,370,901	1,323,502	1,230,315	1,230,315	1,187,644

Notes: As in Table 1, each column shows the effects of climate and job shocks on voter demand from separate regressions, showing the heterogeneity of the main coefficients by the level of polarization on the environment in neighboring districts. The regressions in columns (3) and (6) instrument for share jobs in OGC and share green jobs with their respective shift-share instruments as described in section 3.2. Standard errors are clustered by block-group and district-year and are shown in parentheses. * $p < .10$, ** $p < .05$, *** $p < .01$.

Table A.9: U.S. House vs. Railroad Commissioners

Dep. var.: Dem-Rep vote share	House	Commissioner	House	Commissioner
	(1)	(2)	(3)	(4)
No. of days temp. above historical mean + 2sd	0.455***	0.497***	0.0210	0.103**
	(0.102)	(0.102)	(0.0442)	(0.0432)
No. of days prec. above historical mean + 2sd	0.0220	0.176**	-0.132**	0.157***
	(0.0869)	(0.0779)	(0.0605)	(0.0580)
Share Brown Jobs	-0.378***	-0.462***	0.0250	-0.135*
	(0.127)	(0.134)	(0.0673)	(0.0720)
Share Green Jobs	0.655	1.264***	-0.447	0.696**
	(0.490)	(0.464)	(0.294)	(0.279)
Commissioner vote share			0.872***	
			(0.0120)	
House vote share				0.867***
				(0.0204)
District x Year FE	X	X	X	X
Block group FE	X	X	X	X
Controls	Long	Long	Long	Long
Observations	92,733.000	92,733.000	92,733.000	92,733.000

Notes: This table presents estimates of the Democratic-Republican vote share for U.S. House and Texas Railroad Commissioner elections (2002–2020, excluding 2012). The regressors include climate shocks (temperature and precipitation anomalies) and employment shares in oil, gas, and green jobs. District × year FE is used where appropriate, given the localized nature of House elections. Observations are limited to competitive districts. Standard errors are clustered at the district × year and block group levels.

Table A.10: Structural Parameter Estimates with Control Variables

Name	Estimate	Std Error	Z-value	P-value	Effects
			Democrat's Supply		
λ^d_{temp}	0.0018	0.0011	1.6166	0.1060	0.0144
λ^d_{prec}	0.0015	0.0014	1.1009	0.2709	0.0098
λ^d_G	-0.1256	0.1114	-1.1279	0.2594	-0.0487
λ^d_B	0.0252	0.0300	0.8386	0.4017	0.0284
$\Omega^d_{log_emp}$	0.2731	0.2211	1.2351	0.2168	0.0749
$\Omega^d_{mean_ln_income_all}$	-0.3099	0.1549	-2.0004	0.0455	-0.0809
$\Omega^d_{log_voting_age_pop}$	-0.1762	0.2846	-0.6190	0.5359	-0.0364
β^d	-0.0189	0.0122	-1.5476	0.1217	-0.6050
π^d	0.1751	0.0772	2.2689	0.0233	0.0404
			Republican's Supply		
λ^r_{temp}	-0.0008	0.0015	-0.5507	0.5818	-0.0064
λ^r_{prec}	0.0005	0.0021	0.2511	0.8018	0.0034
λ^r_G	0.0962	0.1038	0.9262	0.3543	0.0373
λ^r_B	-0.0101	0.0248	-0.4058	0.6849	-0.0114
$\Omega^r_{log_emp}$	0.0538	0.1676	0.3210	0.7482	0.0148
$\Omega^r_{mean_ln_income_all}$	-0.4507	0.2274	-1.9818	0.0475	-0.1176
$\Omega^r_{log_voting_age_pop}$	-0.0009	0.3196	-0.0027	0.9978	-0.0002
β^r	0.0034	0.0014	2.4480	0.0144	0.1092
π^r	0.1940	0.0601	3.2296	0.0012	0.0539
			District-level Demand		
δ_{temp}	0.0826	0.0244	3.3841	0.0007	0.6517
δ_{prec}	0.0433	0.0229	1.8874	0.0592	0.2771
δ_G	0.2295	0.1193	1.9233	0.0545	0.0890
δ_B	-0.3482	0.0919	-3.7886	0.0002	-0.3926
Γ_{log_emp}	-0.4447	0.0872	-5.1010	0.0000	-0.1220
$\Gamma_{mean_ln_income_all}$	4.3396	0.3735	11.6197	0.0000	1.1326
$\Gamma_{log_voting_age_pop}$	-3.3658	0.1673	-20.1210	0.0000	-0.6952
γ^d	24.0721	12.8451	1.8740	0.0609	8.3754
γ^r	-1.1543	1.0891	-1.0598	0.2892	-0.4960

Notes: This table presents parameter estimates from the structural equations for Democrats' environmental policy supply, x^d_{ct}; Republicans' environmental policy supply, x^r_{ct}; and the district-level Democratic vote share, $\bar{y}_{ct}$. Standard errors (in parentheses) are clustered by congressional district. z-values and p-values correspond to two-sided tests. The final column ("Marginal Effects") reports the change in the outcome-Democrats' platform in the first panel, Republicans' platform in the second panel, and Democrats' vote share (on a 0-100 scale) in the third panel-resulting from a one-standard deviation increase in the corresponding regressor. Estimation follows a two-step GMM approach, using instruments $\overline{\mathbf{V}}_{ct}, z^d_{ct}, z^r_{ct}$ and weighting by the inverse variance of the estimated district-by-year fixed effects in the first step.

Table A.11: Placebo Structural Estimation Using Only Cultural Ideal Points

Name	Estimate	Std Error	Z-value	P-value	Effects
			Democrat's Supply		
λ^d_{temp}	0.0018	0.0010	1.7908	0.0733	0.0142
λ^d_{prec}	-0.0015	0.0016	-0.9487	0.3428	-0.0096
λ^d_G	0.0456	0.0964	0.4729	0.6363	0.0147
λ^d_B	0.0761	0.0525	1.4495	0.1472	0.0804
β^d	0.0000	0.0084	0.0010	0.9992	0.0003
π^d	0.0856	0.0508	1.6856	0.0919	0.0264
			Republican's Supply		
λ^r_{temp}	-0.0005	0.0013	-0.4018	0.6878	-0.0042
λ^r_{prec}	0.0006	0.0018	0.3703	0.7112	0.0041
λ^r_G	0.0674	0.1398	0.4823	0.6296	0.0217
λ^r_B	0.0231	0.0312	0.7418	0.4582	0.0244
β^r	0.0051	0.0098	0.5203	0.6029	0.1634
π^r	0.1450	0.0561	2.5858	0.0097	0.0367
			District-level Demand		
δ_{temp}	0.0828	0.0245	3.3789	0.0007	0.6533
δ_{prec}	0.0443	0.0231	1.9190	0.0551	0.2789
δ_G	0.2160	0.1174	1.8389	0.0660	0.0696
δ_B	-0.3562	0.0927	-3.8428	0.0001	-0.3762
γ^d	2.0919	7.7269	0.2707	0.7866	0.9109
γ^r	-2.7783	8.8367	-0.3144	0.7532	-1.0642

Notes: This table presents parameter estimates from the structural equations for Democrats' policy supply (cultural issues excluding environmental issues), x^d_{ct}; Republicans' policy supply (cultural issues excluding environmental issues), x^r_{ct}; and the district-level Democratic vote share, $\bar{y}_{ct}$. Standard errors (in parentheses) are clustered by congressional district. z-values and p-values correspond to two-sided tests. The final column ("Marginal Effects") reports the change in the outcome-Democrats' platform in the first panel, Republicans' platform in the second panel, and Democrats' vote share (on a 0-100 scale) in the third panel-resulting from a one-standard deviation increase in the corresponding regressor. Estimation follows a two-step GMM approach, using instruments $\overline{\mathbf{V}}_{ct}, z^d_{ct}, z^r_{ct}$ and weighting by the inverse variance of the estimated district-by-year fixed effects in the first step.

B Constructing Green and Brown Employment and Corresponding Instruments

Our analysis requires measuring green and brown employment at the block-group-year level for 2000 to 2020. Since our definition of green and brown employment is based on 6-digit NAICS (NAICS6) industries, in order to construct green and brown employment series, we need employment data at the block-group-NAICS6-year level. We construct these series from a combination of various data sources.

B.1 Data Sources

Employment at County-NAICS6-Year Level We obtain employment data at the level of workplace county, NAICS6, and year from two sources. The first is the Census County Business Patterns (CBP) database, which contains annual employment data at the geographic-area-industry level in various detail, down to the county-NAICS6-year level. Because the data are suppressed for most county-NAICS6 series to protect confidentiality, we use an imputed dataset constructed by Eckert et al. (2021) which uses the non-suppressed CBP data at higher levels of aggregation along the geographic and industry dimensions to impute the data. We use their imputed CBP data for 2000 to 2003.

The second source is the BLS Quarterly Census of Employment and Wages (QCEW) database. Similarly to the CBP, the QCEW contains annual employment data at geographic-area-industry level in various detail, down to the county-NAICS6-year level, with the data suppressed for most county-NAICS6 series for confidentiality. We implement an imputation procedure developed in Autor et al. (2024), which, similarly to Eckert et al. (2021), uses the non-suppressed data at higher levels of aggregation to impute the data. We construct imputed QCEW data for 2004 to 2020.

We take several steps to harmonize the data across 2000 to 2020. First, we concord all revisions of NAICS6 codes to 2012 NAICS. This was done in Eckert et al. (2021) for the imputed CBP data by splitting employment equally for NAICS6 that split into multiple 2012 NAICS6. We do the same for our imputed QCEW data. We also concord all county FIPS codes to 2010 FIPS, similarly splitting employment equally for FIPS codes that split into multiple 2010 FIPS. Finally, to harmonize our data series, we calculate the ratio of county-level employment in our imputed QCEW data to the imputed CBP data in 2004. We multiply each county-NAICS6 series in the imputed CBP data for 2000 to 2003 by its county-level ratio.

Employment at Block-Group-NAICS2-Year Level Employment data at the level of residence block-group, NAICS2, and year are from two sources. The first is the 2000 Decennial Census from IPUMS (Manson et al. (2024)). The second is the Census LEHD Origin-Destination Employment Statistics (LODES) Residence Area Characteristics (RAC) dataset at the block-2-digit-NAICS-year level, which we use for 2002 to 2021. For a small number of states that do not have full data series from 2002 to 2021, we carry backward (forward) the first (last) year of data to 2002 (2021).

To harmonize the data across 2000 to 2020, we concord all block-group and block FIPS codes to 2010 FIPS, using population weights to apportion the employment data, and collapse the data at block-group-NAICS2-year level. To harmonize the 2000 Census data with the LODES data for 2002 to 2021, we first train a regression model:

$$Emp_{bkt}^{LODES} = \alpha + \beta Emp_{bkt}^{ACS}$$

where Emp_{bkt}^{LODES} is employment at the level of block-group b, NAICS2 k, and year t as measured in the LODES RAC dataset, and Emp_{bkt}^{ACS} is employment as measured in the American Community Survey (ACS) 5-year estimates dataset. The sample period is 2007 to 2021, when the ACS estimates are available, and we estimate separate models for each 2-digit NAICS. We then use the estimated models to predict $\hat{Emp}_{bk,2000}^{LODES}$ based on the observed 2000 Census data, $Emp_{bk,2000}^{Census}$, and use this predicted LODES employment measure for 2000.

Commuting Flow Data at Block-Group-County-Supersector-Year Level We use commuting flow data from the LODES Origin-Destination (OD) dataset, which measures employment at the level of residence block, workplace block, NAICS supersector (specifically, the three supersectors are "Goods Producing", "Trade, Transportation, and Utilities", and "All Other Services"), and year, and which is available for 2002 to 2020. We concord block FIPS codes to 2010 FIPS, using population weights to apportion the employment data, and collapse the data at the level of residence block-group, workplace county, NAICS supersector, and year.

Green Industries and Industry Share of Green Employment We use a classification of NAICS6 industries that potentially produce green goods and services, as well as estimates of the industry shares of employment in each of these industries that are within green establishments, from the BLS Green Goods and Services (GGS) survey. The GGS was only conducted for 2010 and 2011; we use the 2011 survey which is missing data for slightly fewer industries. The survey sample was stratified mostly at

the NAICS4 level, with some highly environmental industries stratified at the NAICS6 level; to avoid bias due to sample stratification, we use only the industry estimates at NAICS4 level.

B.2 Constructing Green and Brown Employment

We construct green employment at the block-group-year level as follows, where all employment variables additionally have year t subscripts, omitted for brevity:

$$GreenEmp_b = \sum_{i \in G} GreenEmp_{bi},$$

$$GreenEmp_{bi} = \sum_{c \in C(b)} Emp_{b,k(i)} \times \frac{Emp_{bc,l(i)}}{Emp_{b,l(i)}} \times \frac{\gamma_{j(i)} \times Emp_{ci}}{Emp_{c,k(i)}}.$$

$GreenEmp_b$ is green employment at the level of residence block-group b and year t; $GreenEmp_{bi}$ is green employment at the level of block-group b and NAICS6 industry i; G is the set of green industries and $\gamma_{j(i)}$ is the industry share of green employment for NAICS4 $j(i)$ corresponding to NAICS6 i as described above; and c is a county and $C(b)$ the set of counties where residents of block-group b work during the sample period. $Emp_{b,k(i)}$ is employment at the level of residence block-group b, NAICS2 $k(i)$ corresponding to NAICS6 i, which is from the 2000 Census and LODES RAC datasets as described above. $Emp_{bc,l(i)}$ is employment residing in block-group b, working in county c, in NAICS super-sector $l(i)$ corresponding to NAICS6 i, which is from the LODES OD dataset as described above; $Emp_{b,l(i)} = \sum_{c \in C(b)} Emp_{bc,l(i)}$. When data are not available for this variable, we assume all residents of the given block-group-super-sector-year work in the county they reside in. Emp_{ci} is employment at the level of workplace county and NAICS6 i, and is from the CBP and QCEW datasets as described above, and $Emp_{c,k(i)} = \sum_{i \in k(i)} Emp_{ci}$.

Note that our construction of green employment relies on the sufficient assumptions

$$\frac{Emp_{bc,l(i)}}{Emp_{b,l(i)}} = \frac{Emp_{bc,k(i)}}{Emp_{b,k(i)}}$$

$$\frac{\gamma_{j(i)} \times Emp_{ci}}{Emp_{c,k(i)}} = \frac{\gamma_{bcit} \times Emp_{bci}}{Emp_{bc,k(i)}}$$

which must be made due to data availability.

We analogously construct brown employment at the block-group-year level as follows, where all employment variables additionally have year t subscripts omitted for

brevity:

$$BrownEmp_b = \sum_{i \in B} BrownEmp_{bi},$$

$$BrownEmp_{bi} = \sum_{c \in C(b)} Emp_{b,k(i)} \times \frac{Emp_{bc,l(i)}}{Emp_{b,l(i)}} \times \frac{\mathbf{1}(i \in B) \times Emp_{ci}}{Emp_{c,k(i)}}.$$

$BrownEmp_b$ is brown employment at the level of residence block-group b and year t; $BrownEmp_{bi}$ is brown employment at the level of block-group b, NAICS6 industry i, and year t; and B is the set of brown industries, which we define as those involved in oil and gas extraction, coal mining, and their support activities. Specifically, the eight industries are "211111 Crude Petroleum and Natural Gas Extraction," "211112 Natural Gas Liquid Extraction," "212111 Bituminous Coal and Lignite Surface Mining," "212112 Bituminous Coal Underground Mining", "212113 Anthracite Mining," "213111 Drilling Oil and Gas Wells," "213112 Support Activities for Oil and Gas Operations," and "213113 Support Activities for Coal Mining." The rest of the variables and assumptions are as defined previously.

Finally, our analysis uses *shares* of green and brown employment at the block-group-year level, so we divide our constructed measures of green and brown employment by total employment, constructed from the 2000 Census and LODES RAC datasets described above.

B.3 Constructing Instruments

We construct a shift-share instrument for our share of green employment variable as follows:

$$\frac{\widehat{GreenEmp}_{bt}}{Emp_{b,2000}} = \sum_{i \in G} \frac{GreenEmp_{bi,2000}}{Emp_{b,2000}} \times \frac{GreenEmp_{it}}{GreenEmp_{i,2000}}.$$

$\hat{GreenEmp}_{bt}$ is predicted green employment in block-group b and year t; we normalize by dividing by $Emp_{b,2000}$, employment in block-group b in the year 2000. i, G, $GreenEmp_{bi,2000}$, and $Emp_{b,2000}$ are defined and constructed the same way as previously described with the year being 2000. $GreenEmp_{it}$ is green employment in NAICS6 i and year t and is constructed by summing $GreenEmp_{bit}$ over block-groups b.

In our setting, the shares, or exposure weights, of our shift-share instrument are the $\frac{GreenEmp_{bi,2000}}{Emp_{b,2000}}$, and the sum of these shares is not generally equal to one across block-groups, a potential issue in shift-share IV regressions highlighted by Borusyak, Hull and Jaravel (2022). We implement the proposed solution in Borusyak, Hull and

Jaravel (2022), which is to control for the sum of shares in our IV regressions. The sum of shares $\frac{GreenEmp_{bi,2000}}{Emp_{b,2000}}$ is simply the share of green employment in block-group b in 2000.

We construct a shift-share instrument for our share of brown employment variable analogously.

C Political Competition Over Environmental Policy

This appendix presents a simple microfoundation for the system of equations estimated in Section 4 of the paper. Our empirical model is more general than the stylized model of political competition presented here, but the economic intuition, identification challenges, and sources of variation used to estimate the empirical model, are all captured by the simple model.

We consider an election between two candidates, D and R. There is a continuum of voters, indexed by i, with their distribution described by the density function $f(i)$. Each voter has an ideal policy point in a multi-dimensional policy space, denoted by the vector θ_i. A voter's utility from a given policy platform $\mathbf{x}$ decreases with the squared Euclidean distance between the platform and their ideal point:

$$u_i(\mathbf{x}) = -\|\mathbf{x} - \theta_i\|^2$$

A voter chooses Candidate D if the total utility from D exceeds that from R. The comparison includes policy utility, a candidate-specific valence term, and a voter-specific idiosyncratic shock.

C.1 Candidates and Voting Probability

Candidates D and R simultaneously choose policy platforms $\mathbf{x}_D$ and $\mathbf{x}_R$. We assume Candidate D has a net non-policy valence advantage over Candidate R, denoted by $\bar{\delta}$. This term is known to all agents. The utility for voter i from Candidate D is $u_i(\mathbf{x}_D) + \bar{\delta} + \epsilon_i$, and from Candidate R is $u_i(\mathbf{x}_R)$. The term ϵ_i is an idiosyncratic shock, assumed to be drawn from a uniform distribution with mean 0 and density ϕ_i. The parameter ϕ_i measures the sensitivity of voter i to policy changes; a high ϕ_i denotes a swing voter.

The probability that voter i votes for Candidate D is:

$$p_i(\mathbf{x}_D, \mathbf{x}_R) = \Pr(\epsilon_i > u_i(\mathbf{x}_R) - u_i(\mathbf{x}_D) - \bar{\delta}) = \frac{1}{2} + \phi_i[u_i(\mathbf{x}_D) - u_i(\mathbf{x}_R) + \bar{\delta}]$$

Candidate D's aggregate expected vote share, Π_D, is the integral over all voters:

$$\Pi_D = \int p_i(\mathbf{x}_D, \mathbf{x}_R) f(i)\, di.$$

Candidates care about both winning and the policy they advocate for during a campaign. Each candidate $J \in \{D, R\}$ has an ideal policy point, $\theta_J = \tilde{\theta}_J + \zeta_J \mathbf{z}_J$ where $\tilde{\theta}$ is the personal preference of the candidate and $\mathbf{z}$ the local party delegation preferences, with a relative weight to the party given by $\zeta \in [0, 1]$. We assume the candidate's objective function V_J is a weighted sum of their expected vote share (office motivation) and their proximity to their ideal policy (policy motivation), with the latter being a composite of both personal and party factors. The weight $\lambda_J \in [0, 1]$ captures the overall importance of policy goals.

For Candidate D, the objective is:

$$V_D(\mathbf{x}_D) = (1 - \lambda_D)\Pi_D - \lambda_D \|\mathbf{x}_D - \theta_D\|^2$$

and for Candidate R, the objective is (since $\Pi_R = 1 - \Pi_D$):

$$V_R(\mathbf{x}_R) = (1 - \lambda_R)(1 - \Pi_D) - \lambda_R \|\mathbf{x}_R - \theta_R\|^2.$$

C.2 Equilibrium Platforms

We find the equilibrium platforms by solving each candidate's optimization problem, taking the other's platform as given. A Nash Equilibrium is a pair of platforms $(\mathbf{x}_D^*, \mathbf{x}_R^*)$ where neither candidate has an incentive to deviate and all voters vote for their preferred candidate and voters choose optimally.

Candidate D chooses $\mathbf{x}_D$ to maximize V_D. Let us analyze the k-th dimension of the policy vectors, say the environmental policy dimension. The first-order condition for a policy dimension x_{Dk} sets:.

$$\begin{aligned}\frac{\partial V_D}{\partial x_{Dk}} &= (1 - \lambda_D)\frac{\partial \pi_D}{\partial x_{Dk}} - \frac{\partial}{\partial x_{Dk}}\left(\lambda_D \sum_j (x_{Dj} - \theta_{Dj})^2\right) = 0 \\ &= (1 - \lambda_D)\frac{\partial \pi_D}{\partial x_{Dk}} - 2\lambda_D(x_{Dk} - \theta_{Dk}) = 0\end{aligned}$$

The partial derivative of the vote share Π_D is:

$$\begin{aligned}
\frac{\partial \Pi_D}{\partial x_{Dk}} &= \int \phi_i \frac{\partial u_i(\mathbf{x}_D)}{\partial x_{Dk}} f(i)\, di \\
&= \int \phi_i \frac{\partial}{\partial x_{Dk}} \left(-\sum_j (x_{Dj} - \theta_{ij})^2 \right) f(i)\, di \\
&= \int \phi_i [-2(x_{Dk} - \theta_{ik})] f(i)\, di \\
&= -2 \left(x_{Dk} \int \phi_i f(i)\, di - \int \theta_{ik} \phi_i f(i)\, di \right)
\end{aligned}$$

Let us define the average policy responsiveness $\bar{\phi} = \int \phi_i f(i)\, di$ and the weighted-mean voter ideal point $\bar{\theta}_k^{\phi} = \dfrac{\int \theta_{ik} \phi_i f(i)\, di}{\bar{\phi}}$. Then:

$$\frac{\partial \Pi_D}{\partial x_{Dk}} = -2\bar{\phi}(x_{Dk} - \bar{\theta}_k^{\phi})$$

Substituting this back into the FOC:

$$\begin{aligned}
(1 - \lambda_D)[-2\bar{\phi}(x_{Dk} - \bar{\theta}_k^{\phi})] - 2\lambda_D(x_{Dk} - \theta_{Dk}) &= 0 \\
x_{Dk}[(1 - \lambda_D)\bar{\phi} + \lambda_D] &= (1 - \lambda_D)\bar{\phi}\bar{\theta}_k^{\phi} + \lambda_D \theta_{Dk} \\
x_{Dk}^* &= \frac{(1 - \lambda_D)\bar{\phi}\bar{\theta}_k^{\phi} + \lambda_D \theta_{Dk}}{(1 - \lambda_D)\bar{\phi} + \lambda_D}
\end{aligned}$$

Candidate R chooses $\mathbf{x}_R$ to maximize V_R, which is equivalent to minimizing $(1 - \lambda_R)\Pi_D + \lambda_R \|\mathbf{x}_R - \theta_R\|^2$. The solution gives:

$$x_{Rk}^* = \frac{(1 - \lambda_R)\bar{\phi}\bar{\theta}_k^{\phi} + \lambda_R \theta_{Rk}}{(1 - \lambda_R)\bar{\phi} + \lambda_R}.$$

The equilibrium policy platforms are given by the solutions to the FOCs. In vector notation and making explicit the components of θ_J we have:

$$\mathbf{x}_D^* = \frac{(1 - \lambda_D)\bar{\phi}\bar{\theta}^{\phi} + \lambda_D \left(\tilde{\theta}_D + \zeta_D \mathbf{z}_D \right)}{(1 - \lambda_D)\bar{\phi} + \lambda_D} \tag{9}$$

$$\mathbf{x}_R^* = \frac{(1 - \lambda_R)\bar{\phi}\bar{\theta}^{\phi} + \lambda_R \left(\tilde{\theta}_R + \zeta_R \mathbf{z}_R \right)}{(1 - \lambda_R)\bar{\phi} + \lambda_R} \tag{10}$$

Note that policy platforms diverge as long as candidates have different ideal points

$(\theta_D \neq \theta_R)$ and care about policy $(\lambda_D, \lambda_R > 0)$. Each candidate's platform is a compromise, a weighted average of the electoral center $(\bar{\theta}^{\phi})$, their personal ideal point $(\tilde{\theta}_J)$, and the local party preferences $(\mathbf{z}_J)$. These equations are a possible (but not the sole) microfoundation of equations (4) and (5) in the text.

C.3 Equilibrium Vote Shares

With divergent platforms, the election outcome depends on both valence and policy positioning. The equilibrium vote share for Candidate D is:

$$\begin{aligned}
\Pi_D^* &= \int \left(\frac{1}{2} + \phi_i [u_i(\mathbf{x}_D^*) - u_i(\mathbf{x}_R^*) + \bar{\delta}] \right) f(i)\, di \\
&= \frac{1}{2} + \bar{\delta} \int \phi_i f(i)\, di + \int \phi_i [u_i(\mathbf{x}_D^*) - u_i(\mathbf{x}_R^*)] f(i)\, di \\
&= \frac{1}{2} + \bar{\delta}\bar{\phi} + \int \phi_i [\|\mathbf{x}_R^* - \theta_i\|^2 - \|\mathbf{x}_D^* - \theta_i\|^2] f(i)\, di
\end{aligned}$$

We can simplify the policy-dependent term in the integral:

$$\begin{aligned}
&\int \phi_i [\|\mathbf{x}_R^* - \theta_i\|^2 - \|\mathbf{x}_D^* - \theta_i\|^2] f(i)\, di \\
&= \int \phi_i [(\|\mathbf{x}_R^*\|^2 - 2\mathbf{x}_R^* \cdot \theta_i + \|\theta_i\|^2) - (\|\mathbf{x}_D^*\|^2 - 2\mathbf{x}_D^* \cdot \theta_i + \|\theta_i\|^2)] f(i)\, di \\
&= \int \phi_i [\|\mathbf{x}_R^*\|^2 - \|\mathbf{x}_D^*\|^2 - 2(\mathbf{x}_R^* - \mathbf{x}_D^*) \cdot \theta_i] f(i)\, di \\
&= (\|\mathbf{x}_R^*\|^2 - \|\mathbf{x}_D^*\|^2)\bar{\phi} - 2(\mathbf{x}_R^* - \mathbf{x}_D^*) \cdot (\bar{\phi}\bar{\theta}^{\phi}) \\
&= \bar{\phi} [\|\mathbf{x}_R^* - \bar{\theta}^{\phi}\|^2 - \|\mathbf{x}_D^* - \bar{\theta}^{\phi}\|^2]
\end{aligned}$$

This gives us the vote share defining our demand function:

$$\Pi_D^* = \frac{1}{2} + \underbrace{\bar{\phi}\bar{\delta}}_{\text{D Valence Advantage}} + \underbrace{\bar{\phi} \left[\|\mathbf{x}_R^* - \bar{\theta}^{\phi}\|^2 - \|\mathbf{x}_D^* - \bar{\theta}^{\phi}\|^2 \right]}_{\text{D Policy Advantage}} \tag{11}$$

or

$$y^* = 2 * \underbrace{\bar{\phi}\bar{\delta}}_{\text{D Valence Advantage}} + 2 * \underbrace{\bar{\phi} \left[\|\mathbf{x}_R^* - \bar{\theta}^{\phi}\|^2 - \|\mathbf{x}_D^* - \bar{\theta}^{\phi}\|^2 \right]}_{\text{D Policy Advantage}} \tag{12}$$

The vote share is determined by three components: a baseline of 0.5, a bonus from non-policy valence for D, and a policy platform advantage that rewards the candidate whose platform is closer to the electoral center of gravity $(\bar{\theta}^{\phi})$ and the equation for y^* is a possible (but not the sole) microfoundation of equation (8) in the text.

Furthermore, if θ_D, θ_R, $\bar{\theta}^{\phi}$, or $\bar{\delta}$ are all functions of (can all be influenced by) the weather and jobs changes $\mathbf{V}$ in our empirical analysis, this model shows why controlling for θ_D and θ_R is important for recovering the direct effect of shocks on voter preferences, given by $\frac{d\Pi_D}{d\bar{\theta}^{\phi}} \times \frac{d\bar{\theta}^{\phi})}{d\mathbf{V}}$, in equation (3), which is why the within-district-by-year variation is important for recovering the effect of demand.

Similarly, the supply equations show that controlling for $\bar{\theta}^{\phi}$ (e.g. voter demand) is important for recovering the *direct* effect of climate on party ideal points $\frac{d\mathbf{x}_J^*}{d\theta_J} \times \frac{d\theta_J}{d\mathbf{V}}$.

The demand model makes an auxiliary prediction, which is that demand shocks to $\bar{\theta}^{\phi}$ will interact with $\theta_R - \theta_D$ due to the nonlinearity implied by the distance function. While we do not observe $\tilde{\theta}_R$ and $\tilde{\theta}_D$ directly, our identification, through the lens of the model, assumes that the instruments $\mathbf{z}_D$ and $\mathbf{z}_R$, operate solely through θ_D and θ_R, once demand is controlled for, and we can use this variation to test for the predicted heterogeneity.

The model further clarifies that candidate ideal points (θ_J) are *not* the observed environmental policy positions of the candidates ($\mathbf{x}_J$), which are endogenous functions of both voter demand and candidate partisan preferences (the ideal points). For this reason, we use our supply-side instruments to form exogenous shifters for the candidate ideology.

D Proof of Identification

This appendix establishes point identification of the structural parameters in the joint demand–supply model for climate-policy platforms (see Section 4 of the main text). Our proof does not invoke second-order moment conditions; imposing those conditions renders the system over-identified.

D.1 Setup and key equations

Our political supply equations (see equations (4) and (5) in the main text) can be written as:

$$x_{ct}^d = \lambda^d \bar{\mathbf{V}}_{ct} \; + \; \beta^d \bar{y}_{ct} \; + \; \pi^d z_{ct}^d \; + \; \omega_c^d \; + \; \zeta_t^d \; + \; \eta_{ct}^d, \tag{13}$$

$$x_{ct}^r = \lambda^r \bar{\mathbf{V}}_{ct} \; + \; \beta^r \bar{y}_{ct} \; + \; \pi^r z_{ct}^r \; + \; \omega_c^r \; + \; \zeta_t^r \; + \; \eta_{ct}^r, \tag{14}$$

where

- x_{ct}^d and x_{ct}^r are the policy positions (e.g., climate platforms) of the Democratic

and Republican candidates in congressional district c at election year t;

- $\bar{\mathbf{V}}_{ct}$ is the (population-weighted) average of exogenous district-level characteristics, such as weather shocks or green/brown employment share;
- $\bar{y}_{ct}$ is the (population-weighted) average of Democratic vote margins in district c (i.e. the expected support) at time t;
- z^d_{ct} and z^r_{ct} are exogenous party-specific shifters (e.g., local party trends) that affect only the Democrat's or the Republican's platform, respectively;
- ω^p_c and ζ^p_t are district and time fixed effects (indexed by party $p \in \{d, r\}$);
- η^p_{ct} are idiosyncratic errors.

On the demand side, aggregating equation (6) from the main text to the district level (as in (8)), we have:

$$\bar{y}_{ct} \;=\; \delta\, \bar{\mathbf{V}}_{ct} \;+\; \gamma^d\, x^d_{ct} \;+\; \gamma^r\, x^r_{ct} \;+\; \nu_c \;+\; \kappa_t \;+\; \xi_{ct}, \tag{15}$$

where δ captures the direct impact of exogenous covariates $\bar{\mathbf{V}}_{ct}$ on vote margins, γ^d and γ^r measure how the Democrat's and Republican's platforms shift the average Democratic vote margin, ν_c and κ_t are district and time fixed effects, and ξ_{ct} is an error term.

We are interested in identifying the structural parameters:

$$\big\{\, \beta^d,\, \beta^r,\, \gamma^d,\, \gamma^r,\, \pi^d,\, \pi^r,\, \lambda^d,\, \lambda^r,\, \delta \big\}.$$

Below, we show how these parameters can be uniquely recovered from appropriate *first-order* (linear) moment conditions, which underlie the GMM approach detailed in Section 4 of the main text.

D.2 Reduced-Form Relationships

Recall the structural equations for our demand and supply system at the district level:

$$\begin{aligned}
\bar{y}_{ct} &= \delta\, \bar{\mathbf{V}}_{ct} \;+\; \gamma^d\, x^d_{ct} \;+\; \gamma^r\, x^r_{ct} \;+\; \nu_c \;+\; \kappa_t \;+\; \xi_{ct}, \\
x^d_{ct} &= \lambda^d\, \bar{\mathbf{V}}_{ct} \;+\; \beta^d\, \bar{y}_{ct} \;+\; \pi^d\, z^d_{ct} \;+\; \omega^d_c \;+\; \zeta^d_t \;+\; \eta^d_{ct}, \\
x^r_{ct} &= \lambda^r\, \bar{\mathbf{V}}_{ct} \;+\; \beta^r\, \bar{y}_{ct} \;+\; \pi^r\, z^r_{ct} \;+\; \omega^r_c \;+\; \zeta^r_t \;+\; \eta^r_{ct}.
\end{aligned}$$

Here, $\bar{y}_{ct}$ is the average Democratic vote margin in district c, and x^d_{ct} and x^r_{ct} denote the platforms of the Democratic and Republican candidates, respectively. The variables $\bar{\mathbf{V}}_{ct}$ are exogenous district-level covariates, and z^d_{ct} and z^r_{ct} are party-specific policy shifters. We collect the district and time fixed effects into $\{\nu_c, \kappa_t, \omega^d_c, \omega^r_c, \zeta^d_t, \zeta^r_t\}$ and the stochastic terms into $\{\xi_{ct}, \eta^d_{ct}, \eta^r_{ct}\}$.

Because x^d_{ct} and x^r_{ct} each depend on $\bar{y}_{ct}$ (which itself depends on x^d_{ct} and x^r_{ct}), we substitute the demand equation into the supply equations and collect terms. Denote

$$\Xi \;=\; \frac{1}{1 \;-\; \beta^d\,\gamma^d \;-\; \beta^r\,\gamma^r}, \quad \alpha_{ct} \;=\; \nu_c + \kappa_t, \quad \rho^d_{ct} \;=\; \omega^d_c + \zeta^d_t, \quad \rho^r_{ct} \;=\; \omega^r_c + \zeta^r_t,$$

$$\Lambda_{ct} \;=\; \xi_{ct} \;+\; \gamma^d\,\eta^d_{ct} \;+\; \gamma^r\,\eta^r_{ct}.$$

Then we can write the reduced-form expressions as:

$$\begin{aligned}
\bar{y}_{ct} = {}& \Xi\Big(\alpha_{ct} \;+\; \gamma^d \rho^d_{ct} \;+\; \gamma^r \rho^r_{ct}\Big) \;+\; \Xi\Big(\,\delta \;+\; \gamma^d\,\lambda^d + \gamma^r\,\lambda^r\Big)\,\bar{\mathbf{V}}_{ct} \\
& +\; \big(\Xi\,\gamma^d\,\pi^d\big)\,z^d_{ct} \;+\; \big(\Xi\,\gamma^r\,\pi^r\big)\,z^r_{ct} \;+\; \big(\Xi\,\Lambda_{ct}\big), \\
x^d_{ct} = {}& \Big[\rho^d_{ct} \;+\; \beta^d\,\Xi\big(\alpha_{ct} \;+\; \gamma^d \rho^d_{ct} \;+\; \gamma^r \rho^r_{ct}\big)\Big] \;+\; \Big[\lambda^d \;+\; \beta^d\,\Xi\big(\delta + \gamma^d \lambda^d + \gamma^r \lambda^r\big)\Big]\,\bar{\mathbf{V}}_{ct} \\
& +\; \Big[\beta^d\,\Xi\,\gamma^d\,\pi^d \;+\; \pi^d\Big]\,z^d_{ct} \;+\; \beta^d\,\big(\Xi\,\gamma^r\,\pi^r\big)\,z^r_{ct} \;+\; \Big[\beta^d\,\Xi\,\Lambda_{ct} \;+\; \eta^d_{ct}\Big], \\
x^r_{ct} = {}& \Big[\rho^r_{ct} \;+\; \beta^r\,\Xi\big(\alpha_{ct} \;+\; \gamma^d \rho^d_{ct} \;+\; \gamma^r \rho^r_{ct}\big)\Big] \;+\; \Big[\lambda^r \;+\; \beta^r\,\Xi\big(\delta + \gamma^d \lambda^d + \gamma^r \lambda^r\big)\Big]\,\bar{\mathbf{V}}_{ct} \\
& +\; \beta^r\,\big(\Xi\,\gamma^d\,\pi^d\big)\,z^d_{ct} \;+\; \Big[\beta^r\,\Xi\,\gamma^r\,\pi^r \;+\; \pi^r\Big]\,z^r_{ct} \;+\; \Big[\beta^r\,\Xi\,\Lambda_{ct} \;+\; \eta^r_{ct}\Big].
\end{aligned}$$

To see how the system parameters can be recovered from simple linear regressions, consider regressing each district-level outcome on the exogenous instruments $\bar{\mathbf{V}}_{ct}$, z^d_{ct}, and z^r_{ct}, partialling out district and year fixed effects. We define the following reduced-form slopes:

- From the regression of $\bar{y}_{ct}$ on ($\bar{\mathbf{V}}_{ct}$, z^d_{ct}, z^r_{ct}) with district and year fixed effects, let

  $$k_{y,\bar{\mathbf{V}}} \quad k_{y,z^d} \quad \text{and} \quad k_{y,z^r}$$

  denote the estimated coefficients on $\bar{\mathbf{V}}_{ct}$, z^d_{ct} and z^r_{ct}, respectively.

- From the regression of x^d_{ct} on ($\bar{\mathbf{V}}$, z^d_{ct}, z^r_{ct}) with district and year fixed effects, let

  $$k_{x^d,\bar{\mathbf{V}}} \quad k_{x^d,z^d} \quad \text{and} \quad k_{x^d,z^r}$$

denote the estimated coefficients on $\bar{\mathbf{V}}_{ct}$, z^d_{ct} and z^r_{ct}, respectively.

- Similarly, from the regression of x^r_{ct} on ($\bar{\mathbf{V}}_{ct}$, z^d_{ct}, z^r_{ct}) with district and year fixed effects, let

$$k_{x^r,\bar{\mathbf{V}}} \quad k_{x^r,z^d} \quad \text{and} \quad k_{x^r,z^r}$$

denote the estimated coefficients on $\bar{\mathbf{V}}_{ct}$, z^d_{ct} and z^r_{ct}, respectively.

Reduced-Form Expressions. From the algebraic derivations here, we obtain:

$$\begin{aligned}
k_{x^d,\bar{\mathbf{V}}} &= \lambda^d + \beta^d \Xi \left(\delta + \gamma^d \lambda^d + \gamma^r \lambda^r\right) \\
k_{x^d,z^d} &= \beta^d \Xi \gamma^d \pi^d + \pi^d = \Xi \left[\pi^d - \pi^d \beta^r \gamma^r\right], \\
k_{x^d,z^r} &= \Xi \left[\pi^r \beta^d \gamma^r\right], \\
k_{x^r,\bar{\mathbf{V}}} &= \lambda^r + \beta^r \Xi \left(\delta + \gamma^d \lambda^d + \gamma^r \lambda^r\right) \\
k_{x^r,z^d} &= \Xi \left[\pi^d \beta^r \gamma^d\right], \\
k_{x^r,z^r} &= \beta^r \Xi \gamma^r \pi^r + \pi^r = \Xi \left[\pi^r - \pi^r \beta^d \gamma^d\right], \\
k_{y,\bar{\mathbf{V}}} &= \Xi(\delta + \gamma^d \lambda^d + \gamma^r \lambda^r) \\
k_{y,z^d} &= \Xi \gamma^d \pi^d, \\
k_{y,z^r} &= \Xi \gamma^r \pi^r,
\end{aligned}$$

where

$$\Xi = \frac{1}{1 - \beta^d \gamma^d - \beta^r \gamma^r}.$$

Hence, all reduced-form slopes $\{k_{x^d,\bar{\mathbf{V}}}, k_{x^d,z^d}, k_{x^d,z^r}, k_{x^r,\bar{\mathbf{V}}} k_{x^r,z^d}, k_{x^r,z^r}, k_{y,\bar{\mathbf{V}}}, k_{y,z^d}, k_{y,z^r}\}$ are functions of the structural parameters $\left\{\beta^d, \beta^r, \gamma^d, \gamma^r, \pi^d, \pi^r, \lambda^d, \lambda^r, \delta\right\}$.

D.3 Recovering the Structural Parameters

Solving these equations for the unknowns structural parameters yields a unique solution (provided that Ξ is well-defined). In particular:

$$\begin{aligned}
\beta^d &= \frac{k_{x^d,z^r}}{k_{y,z^r}}, \qquad \beta^r = \frac{k_{x^r,z^d}}{k_{y,z^d}}, \\
\gamma^d &= -\frac{k_{x^r,z^d} k_{y,z^r} - k_{x^r,z^r} k_{y,z^d}}{k_{x^d,z^d} k_{x^r,z^r} - k_{x^d,z^r} k_{x^r,z^d}}, \quad \gamma^r = \frac{k_{x^d,z^d} k_{y,z^r} - k_{x^d,z^r} k_{y,z^d}}{k_{x^d,z^d} k_{x^r,z^r} - k_{x^d,z^r} k_{x^r,z^d}}, \\
\pi^d &= \frac{k_{x^d,z^d} k_{y,z^r} - k_{x^d,z^r} k_{y,z^d}}{k_{y,z^r}}, \qquad \pi^r = -\frac{k_{x^r,z^d} k_{y,z^r} - k_{x^r,z^r} k_{y,z^d}}{k_{y,z^d}}.
\end{aligned}$$

Similarly, the expressions for λ^d and λ^r are:

$$\lambda^d = k_{x^d,\bar{\mathbf{V}}} - \frac{k_{y,\bar{\mathbf{V}}} k_{x^d,z^r}}{k_{y,z^r}}$$
$$\lambda^r = k_{x^r,\bar{\mathbf{V}}} - \frac{k_{y,\bar{\mathbf{V}}} k_{x^r,z^d}}{k_{y,z^d}}$$

and finally the expression of δ can be expressed as:

$$\delta = k_{y,\bar{\mathbf{V}}}(1 - \beta^d\gamma^d - \beta^r\gamma^r) - \gamma^d\lambda^d - \gamma^r\lambda^r$$

Hence, using the direct reduced-form coefficients

$$\{k_{x^d,\bar{\mathbf{V}}}, k_{x^d,z^d}, k_{x^d,z^r}, k_{x^r,\bar{\mathbf{V}}}, k_{x^r,z^d}, k_{x^r,z^r}, k_{y,\bar{\mathbf{V}}}, k_{y,z^d}, k_{y,z^r}\}$$

we can recover the entire set of structural demand and supply parameters

$$\left\{\beta^d, \beta^r, \gamma^d, \gamma^r, \pi^d, \pi^r, \lambda^d, \lambda^r, \delta\right\}.$$

In the estimation presented in the main text, we extend this point-identifiable model in two ways. First, given that we observe voting margins, climate shocks, and employment shifts at a more granular block level, we employ block-group-level regression to estimate the parameters δ in the first stage. This approach yields greater precision compared to relying solely on district-level variations. Second, we impose additional second-order moment conditions to restrict the dependence structure between the demand side and the idiosyncratic errors on both parties' supply sides. These two extensions enhance the precision of the estimation and render the system over-identified.